2023

Unique Lactobacillus Produced Metabolites Modulate T-Cell Response through the Aryl Hydrocarbon Receptor: Implications for CNS Autoimmunity

Eamonn Ray Heney
The University of Vermont

Unique *Lactobacillus* Produced Metabolites Modulate T-Cell Response through the Aryl Hydrocarbon Receptor: Implications for CNS Autoimmunity

Eamonn Heney

Undergraduate Honors Thesis

Krementsov Lab

April, 2023

Abstract

Multiple Sclerosis (MS) is an autoimmune disease that affects the central nervous system (CNS). The causes of MS are extremely complex; however, it's becoming increasingly apparent that disease risk is highly associated with environmental factors and consequent gene-environmental interactions. As such, this study focuses on the connection between the gut microbiome and CNS as an arising risk factor and potential mediator of CNS autoimmune disease. The present research examines the capacity of a gut commensal species, *Lactobacillus reuteri* (*L. reuteri*), to modulate effector function of immune cells in the peripheral immune system and along the GI tract, before these cells go on to invade the CNS and initiate breakdown of the blood brain barrier (BBB). One proposed mechanism by which *L. reuteri* impacts immune cells is through the production of tryptophan-derived indole metabolites. We hypothesize that these metabolites act as agonists for the aryl hydrocarbon receptor (AhR), and through modulating the AhR, enhance pathogenic immune responses by means of cytokine production to mediate and sustain an inflammatory autoimmune phenotype across the BBB. To test specifically if *L. reuteri* can modulate the immune system through the production of unique metabolites, we treated cultured cell lines and primary T cells with bacterial-produced tryptophan metabolites and monitored the levels of AhR activity directly through a luciferase reporter system or resulting cytokine production through flow cytometry and ELISA. Through these methods, we found that *L. reuteri*-derived metabolites activate the AhR in a ligand-specific manner, with some acting as agonists while others could function as antagonists of the receptor. We also found that an increase in AhR activity correlated with an increase in pro-inflammatory interleukin-17 (IL-17) and interferon-gamma (IFN-γ) cytokines produced by T cells, hinting at a potential mechanistic pathway of enhanced autoimmunity through microbiota-induced AhR activity.

Table of Contents

Introduction

Pathogenesis of MS

Multiple Sclerosis is the most common non-traumatic neurologic disease in young adults, with about 1 million cases in the United States and 2.8 million cases worldwide [1]. MS is characterized by CNS inflammation, myelin sheath degeneration, and weakening of the blood-brain barrier (BBB) [2]. There are competing hypotheses regarding the pathogenesis of MS. The first, dubbed the “inside-out” hypothesis, involves primary cytodegenerative processes within the CNS [3] and is outside the scope of this study. The second, “outside-in” hypothesis is much more relevant to the role of microbiota and this study. In this hypothesis, a periphery immune response is responsible for the MS phenotype [3]. During peripheral immune cell invasion into the CNS, the BBB is weakened, in part, by the downregulation of tight junctional proteins in the endothelium of the BBB, coinciding with the infiltration of autoimmune B cells and T cells, distinctly of the Th1 and Th17 phenotypes. Once across the BBB, there is an interaction between the T cell receptors (TCR) on $CD4^+$ and $CD8^+$ T lymphocytes, and myelin antigens presented by class II or class I major histocompatibility complex (MHC) expressed primarily on dendritic cells but also on macrophages, microglia, and astrocytes. This leads to an immune attack on the myelin-oligodendrocyte complex. The interaction between T cells and myelin antigens also incites a large inflammatory response and the continued proliferation of immune cells, sustaining the secretion of inflammatory mediator cytokines such as IL-17 and IFN-γ. These cytokines are thus a proxy for effector function in the CNS as it pertains to MS pathogenesis. (**Fig. 1**). Symptoms of MS are heterogenous, however, commonly include fatigue, limb weakness, cognitive dysfunction, and depression [4].

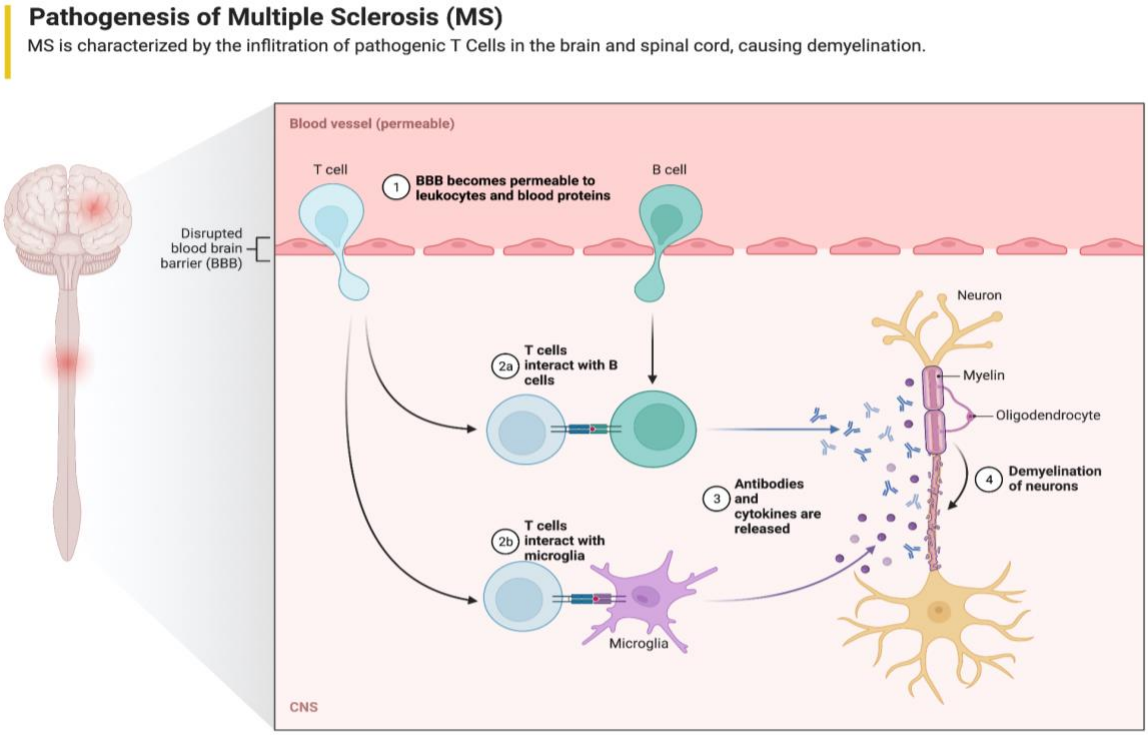

Figure 1. ***Pathogenesis of MS is Characterized by Immune Cell BBB Infiltration***

The pathogenesis of Multiple Sclerosis (MS) begins when T-cells, activated in the periphery, cross the blood-brain barrier, and enter the central nervous system. Once inside the CNS, T-cells initiate an immune response that results in demyelination and axonal damage, leading to the characteristic symptoms of MS (created with Biorender.com).

Role of Microbiota and *L. reuteri* in MS

The etiology of MS is extremely nuanced, with a variety of genetic, environmental, and lifestyle factors that influence the underlying causes of the disease and its clinical presentation. Previous scientific work has illustrated that changes in, or disorder of, the gut microbiome could increase the potential for exacerbation of autoimmune diseases, such as MS, in the genetically predisposed [5,6]. It is proposed that the gut microbiome can influence the immune system through two main modes: through direct interaction with immune cells, or through the production of immunomodulatory metabolites. Bacterial-produced metabolites, including those generated by tryptophan metabolism, have been the focus of clinical research as many of these metabolites have been found in elevated levels in the blood, urine, and other sera of MS patients [7]. In previous studies, the

Krementsov lab has determined that a particular *Lactobacillus* species, *L. reuteri*, is sufficient to exacerbate the severity of experimental autoimmune encephalomyelitis (EAE), a commonly accepted and widely utilized experimental model for MS in mice [6]. EAE is induced by immunization with myelin antigens resulting in lesions of the CNS and demyelination comparable to that of MS. Specifically, in a study by Montgomery et al. (2022), C57BL/6 (B6) mice were colonized with *L. reuteri* from an isolated culture. These mice were then subjected to EAE and were tracked on a 30-day disease course to follow disease progression and severity. This study concluded that mice colonized with *L. reuteri* not only showed EAE symptoms faster than *L. reuteri* free mice, but they also demonstrated a greater severity of disease [6]. In follow-up studies of the same populations, the colonization of *L. reuteri* has repeatedly proven to be sufficient to increase EAE scores and exacerbate autoimmune disease [6].

As a putative probiotic and gut commensal species, *L. reuteri* has a controversial reputation in the literature. In a healthy host, some strains of *L. reuteri* have been found to have many immune-related health benefits such as a decrease in inflammation, strengthening of the intestinal barrier, and a decrease in microbial translocation to distant tissues [8]. Moreover, in the context of CNS autoimmunity, some studies show that *L. reuteri* may ameliorate disease when administered as a probiotic [8,9]. Other studies, however, show the opposite effect where the presence of *L. reuteri* causes exacerbation of CNS autoimmunity [5,6,10]. It may seem counterintuitive that a commensal like *L. reuteri* can play a “pathogenic” role. As a partial explanation for this context dependent role in modulating CNS disease, impact on the immune system can be seen as a double-edged sword. For example, enhancement of T cell responses by this commensal could promote pathogenic effector function in our model, or, alternatively, enhance regulatory T cell responses to tamp down the autoimmunity. Furthermore, while there is no one switch that causes *L. reuteri* to become “pathogenic”, several potential factors can lead to a pathogenic outcome. One such factor is bacterial genetics. For example, while many strains of *E. coli* exist, some strains are pathogenic, causing food-borne illness. Others, however, are non-pathogenic and are essential to mammalian vitamin synthesis. The same logic applies for *L. reuteri*. While some strains are found in common probiotics, others have been associated with increased autoimmunity [5,6,10]. There is also host

genetics to consider. Specifically, genetics control the host's immune system, can alter the abundance of gut microbiome constituents, and more broadly influence host-microbiome interactions [6]. In other words, when investigating previous studies of *L. reuteri,* host genetics need to be considered and may partially account for the disparate findings that riddle the literature.

Proposed Mechanism of Microbiota-Immune Interaction: The AhR

One proposed mechanism as to how a commensal species like *L. reuteri* could impact autoimmune disease involves the AhR. The AhR is an extremely important cytoplasmic ligand-activated transcription factor present in a variety of immune cells, including T cells [11]. In normal immune cells, the AhR is vital to many cellular processes including cellular homeostasis, proliferation, and differentiation. In the context of autoimmunity, however, the AhR could have adverse effects, including effects on BBB integrity [12], the induced transcription of genes that encode for inflammatory cytokines, and driving cells towards a Th17 phenotype. It is thought that indole metabolites or other byproducts of bacterial metabolism produced by gut microbiota can act as ligands for the AhR [13,14]. Specifically, metabolites originating from bacterial tryptophan metabolism seem to be distinct agonists for the AhR (**Fig. 2**). Tryptophan is an essential amino acid that is primarily obtained from the diet of the host. As such, tryptophan is metabolically available to bacteria residing in the GI tract, including *L. reuteri*. Broadly speaking, tryptophan is an amino acid required to make protein for the mammalian host. Tryptophan is also a precursor for the biosynthesis of various important molecules, such as neurotransmitters and signaling molecules. In the context of this study, however, the mammalian and bacterial metabolic byproducts of tryptophan may act as ligands to the AhR. For example, previous study of bacterial tryptophan metabolites found that when *Lactobacilli*, including *L. reuteri*, are given an unrestricted source of tryptophan, they produce the AhR ligand, indole-3-aldehyde (I3A) [14]. The full range of metabolites produced by *Lactobacilli* and their impact on the AhR, however, remains to be elucidated.

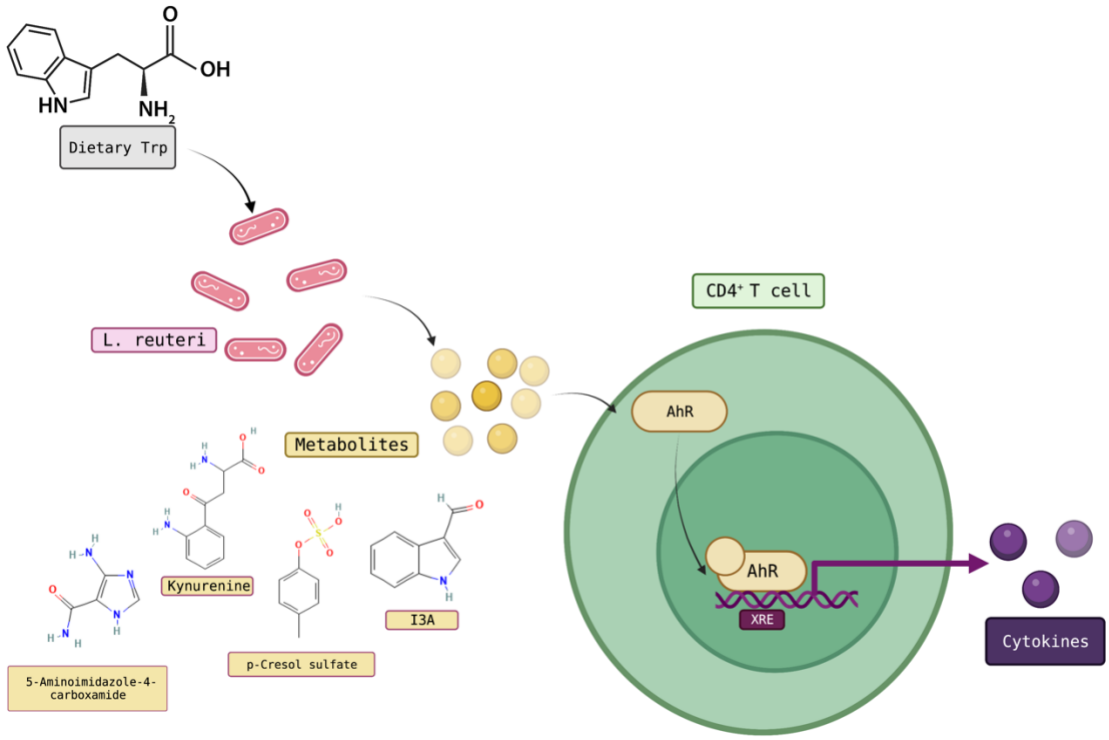

Figure 2. ***The Hypothetical Pathway of AhR Activation by L. reuteri Metabolites***

The proposed pathway by which tryptophan-derived *L. reuteri* metabolites activate the AhR within immune cells, leading to the eventual production of cytokines and increased pathogenesis (created with Biorender.com).

There are 3 main pathways by which tryptophan is metabolized: the kynurenine pathway, the serotonin pathway, and the indole pathway, the latter of which encompasses the uniquely bacterial pathways of tryptophan metabolism. 90% of mammalian tryptophan metabolism occurs through the host kynurenine pathway, where tryptophan is converted into kynurenine by the enzyme tryptophan 2,3-dioxygenase (TDO) or indoleamine 2,3-dioxygenase (IDO). Kynurenine is further metabolized into a number of downstream metabolites such as 3-hydroxykynurenine, quinolinic acid, and kynurenic acid. The balance among these kynurenine pathway metabolites is thought to play a role in MS pathogenesis [15,16,17]. This pathway has also previously been shown to play a role in regulating the immune system and autoimmunity [18]. Furthermore, kynurenine, a suspected AhR agonist, has been found in heightened levels in the serum taken from MS patients [19].

The serotonin pathway of tryptophan metabolism involves several host enzymatic reactions that convert tryptophan to serotonin (5-hydroxytryptamine). Interestingly, 5-hydroxytryptamine levels are reduced in MS patient serum [20,21]. The final pathway of bacterial-derived tryptophan metabolism is the indole pathway, in which tryptophan is converted into various indole derivatives by aromatic amino acid aminotransferase (ArAT) [6]. Many of these derivates, including indole-3-lactate (ILA) and indole-3-acetate (I3A) have been shown in altered levels in MS patient serum [22,23]. Moreover, some of these indole metabolites, such as I3A, have previously been characterized as a part of *L. reuteri* metabolism [6,7]. Many others, however, are novel in the context of *L. reuteri* metabolism and were first characterized in previous study by Montgomery et al. (2022) of the Krementsov lab (**Table 1**). Kynurenine and kynurenate, for example, are traditionally considered canonical mammalian host metabolites but were also found in elevated levels in *L. reuteri* monoculture (**Table 1**).

Table 1. ***Hypothesized Metabolites of Interest that May Act as AhR Ligands***

The hypothesized list of metabolites that may act as AhR ligands, taken from *L. reuteri* monoculture data from Montgomery et al. (2022). Metabolites are broken up into indole, imidazole, cresol, and kynurenine families. The upstream substrate for indole and kynurenine metabolites is tryptophan, while that of imidazoles is traditionally histidine. Some metabolites have been previously shown to be metabolites of *L. reuteri* metabolism (known). Most, however, are novel metabolites yet to be described in *L. reuteri* metabolism (novel).

Metabolite Name	*Family*	*Upstream Substrate*	*Source*	*Known/Novel*
Tryptamine	Indole	Tryptophan	*L. reuteri*	Novel
Indole-3-lactate	Indole	Tryptophan	*L. reuteri*	Known
Indole-3-acetate	Indole	Tryptophan	*L. reuteri*	Known
Indole-3-aldehyde	Indole	Tryptophan	*L. reuteri*	Known
Indole-3-glyoxylic acid	Indole	Tryptophan	*L. reuteri*	Novel
Indole acrylate	Indole	Tryptophan	Bacterial	Novel
Indoxyl glucuronide	Indole	Tryptophan	Bacterial	Novel
Indoxyl-3-sulfate	Indole	Tryptophan	Bacterial	Novel

1-Methyl-4-imidazole acetate	Imidazole	Histidine	*L. reuteri*	Novel
5-Aminoimidazole-4-Carboxamide	Imidazole	Histidine	*L. reuteri*	Novel
4-imidazole acetate	Imidazole	Histidine	*L. reuteri*	Novel
Imidazole propionate	Imidazole	Histidine	*L. reuteri*	Novel
p-Cresol sulfate	Cresol	Tyrosine	*L. reuteri*	Novel
Kynurenine	Kynurenine	Tryptophan	Host	Novel
Kynurenate	Kynurenine	Tryptophan	Host	Novel

Study Objectives

The overarching objective of this study is to assess whether bacterial metabolites produced by *L. reuteri* modulate T-cell response via an AhR-mediated pathway. From monoculture data of *L. reuteri* previously conducted in the Krementsov lab [6], a host of tryptophan-dependent metabolites including I3A, indole-3-glyoxylic acid (IGoxA), and N-acetyl-kynurenine were produced in elevated levels when *L. reuteri* was supplemented with a dietary abundance of tryptophan. In the presence of high tryptophan, *L. reuteri* also produced significant amounts of novel imidazole metabolites as well as a member of a novel cresol metabolite group, p-cresol sulfate. In this study, we hypothesize that tryptophan-derived metabolites, like those previously mentioned, act as agonists for the AhR, leading to the production of pathogenic cytokines in T cells. These cytokines, namely granulocyte macrophage-colony stimulating factor (GM-CSF), IFN-γ, and IL-17 may then induce an inflammatory response within the CNS. As such, we hypothesize that *L. reuteri* has the capacity, in the genetically predisposed, to exacerbate MS autoimmune response through an AhR-mediated pathway.

To assess the mechanism by which *L. reuteri* may impact the AhR, we sought to quantify AhR activity in a luciferase-based reporter system. Specifically, we measured and optimized AhR activity by exposing NIH3T3 (3T3) cells and HEK293T (293T) cells to known strong AhR agonists 6-Formylindolo(3,2-b)carbazole (FICZ) and 2,3,7,8-

Tetrachlorodibenzo-p-dioxin (TCDD), both with and without the presence of a known AhR inhibitor, CH-223191, in a novel dual plasmid reporter system [6]. Both FICZ and TCDD are known high affinity agonists for the AhR that stimulate a strong AhR response [24]. In this assay, cells were transfected with a plasmid encoding the AhR protein (pAhR) and a second reporter plasmid, pGud-Luc, that contains a series of DNA binding elements specific to the AhR known as drug-responsive elements (DREs). These DREs mimic what would happen naturally in the cell, where the intracellular AhR receptor binds to an agonist to become active. It then translocates to the nucleus to bind to specific Xenobiotic response elements (XREs) in the DNA to function as a transcription factor. In the cell, this is how cytokine production would be modulated. In the case of pGud-Luc, a gene that encodes for luciferase is transcribed as a surrogate for AhR activity (**Fig. 3**). When provided with luciferin, luciferase mediates an oxidation reaction where light is formed as a byproduct. AhR activity can, therefore, be measured via luminescence and quantified using a luminometer.

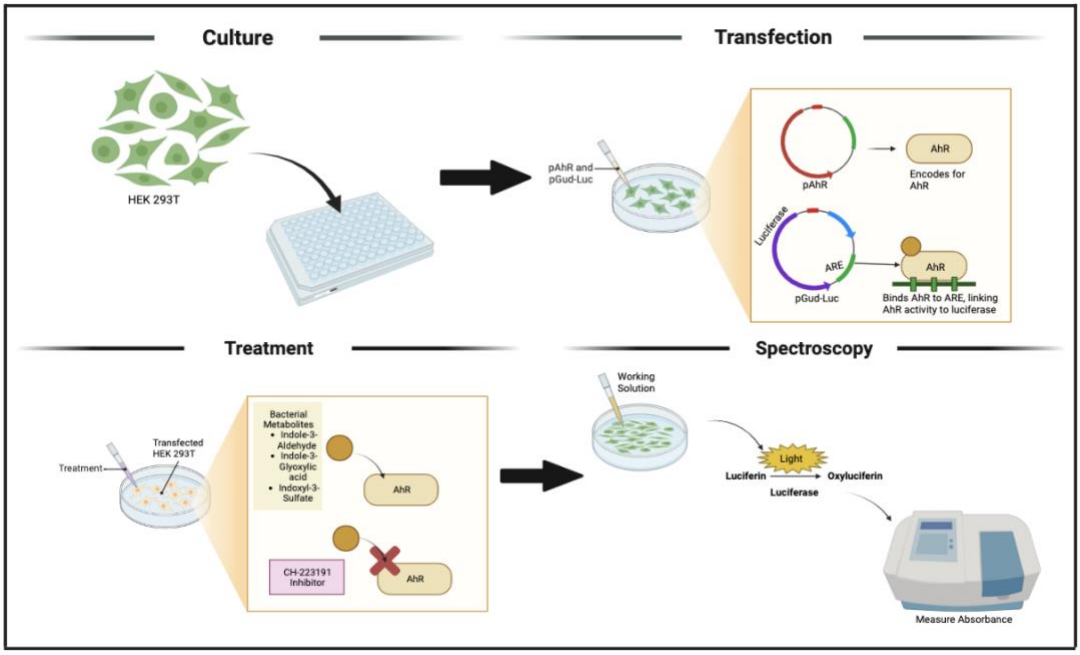

Figure 3. ***Depiction of the Luciferase Reporter System in Four Steps***

A depiction of the Luciferase Assay, from the culture of HEK293T cells to spectroscopy and measuring the absorbance. The assay involves 4 main steps: Culture, Transfection, Treatment, and Spectroscopy, all of which are conducted over a 5-day period. The overarching goal of this assay is to quantify AhR activity within the cell by tying the AhR to luciferase (note the transfection step), which undergoes an oxidation reaction in the presence of Luciferin (step 4), producing light as a byproduct that can be read on a

luminometer. The quantified measure of the AhR can then be experimentally manipulated with various *L. reuteri*-derived metabolites (step 3) (created with Biorender.com).

Summary of Major Results and Broader Implications

Metabolites taken from *L. reuteri* monoculture data (**Table 1**) were found to activate the AhR through the cell-based luciferase assay. In many instances, these metabolites activated the AhR comparably to known high affinity agonists TCDD and FICZ. That having been said, these *L. reuteri*-derived metabolites acted at the AhR in divergent and unique ways, with some metabolites acting as strong AhR agonists while others inhibited receptor activity. Moreover, through flow cytometry, we found that these metabolites alter IL-17 production in primary T cells in vitro. The direction of alteration to IL-17 production was parallel to the metabolites effect on the AhR. Notably, the experimentally determined AhR antagonist and *L. reuteri* metabolite, p-cresol sulfate, inhibited IL-17 production. Its inhibitory capacity was defined by its ability to tamp down strong IL-17 production in response TCDD treatment, a high affinity AhR agonist. Compellingly, this effect had the highest association in $CD8^+$ T cells, which is consistent to what is seen in MS patients, who typically have a relatively stronger $CD8^+$ driven immune response [25,26]. Taken together, our data illustrate a mechanism not unlike a double-edged sword in which *L. reuteri* derived metabolites have divergent agonistic and antagonistic effects on the AhR and subsequent cytokine production. These data highlight that *L. reuteri*-host interactions may modulate the immune system, affecting CNS autoimmunity. Broadly, these data help uncover another piece of the dynamic relationship between the gut microbiome and the immune system and act to fill gaps in the current literature by connecting species-specific interactions of the gut microbiome to immune cells in the CNS via an AhR-dependent mechanism.

Methods

1. Cell-Based Luciferase Dual Plasmid Reporter System

A. Optimization of the Luciferase System

A luciferase dual plasmid system, which tied AhR activity of any particular cell to luminescence via a luciferase-mediated reaction (**Fig. 3**), was run over the course of five days. First, both NIH3T3 (3T3) cells and HEK293T (293T) cells were seeded in respective 96-well cell culture plates at a confluence of 20,000 cells per well in DMEM High Glucose medium consisting of 10% fetal bovine serum (FBS) and 1% Sodium Pyruvate (NaPy). Cells were allowed to adhere and grow for 24 hours in an incubator at 37°C with 5% $C0_2$ until confluency was reached.

At confluency, cells were transfected via a dual plasmid system as follows: Dilutions of Opti-MEM reduced serum media and lipofectamine (0.1 ng/µl) were made and were combined in a 1:1 ratio with a dilution containing the AhR plasmid (pAhR) (240.7ng/µl) and pGud-Luc (386.3 ng/µl). The combined plasmid-lipid complex was then added to the 96-well plates containing the 3T3 and 293T cells (**Fig.3**). After a 24-hour incubation period, cells were pre-treated with or without the CH-223191 AhR inhibitor (10µM) in DMEM High Glucose cell medium with 10% FBS and 1% NaPy for 4 hours.

For agonist treatments, dilution curves of known AhR agonists FICZ and TCDD were made in 4 separate dilutions (0.0176 mM, 0.00176 mM, 0.000176 mM, and 0.0000176 mM) in 3T3 and 293T cells. Controls included treatment with phosphate-buffered saline (PBS) and dimethyl sulfoxide (DMSO) at a matched dilution series to experimental treatments to account for any vehicle-induced effects on the AhR from FICZ and TCDD. 48 hours post-treatment, cells were lysed with the provided lysis buffer in the Pierce Firefly Luciferase Glow Assay Kit (Thermo Fisher, USA) followed by addition D-Luciferin diluted at 1:1000 in working solution also provided in the kit (**Fig. 3**). Luciferase activity was measured using a luminometer at an absorbance of 480 nm. The absorbance data were analyzed using an ANOVA of 2 technical replicates per group in both Prism 9 and Microsoft Excel. The results were compared between treatment groups and control groups to determine significant differences.

B. Luciferase Assay with Bacterial Metabolites

The luciferase assay was conducted in the exact same fashion as the previously described optimization with FICZ and TCDD. Bacterial metabolites were chosen based on metabolites produced by *L. reuteri* in monoculture as described by Montgomery et al. (2020). Specific metabolites of focus included I3A, indoxyl-3-sulfate (I3S), and p-cresol sulfate, among others. 293T cells were exposed to each metabolite in a series of 10-fold dilutions of 100 μM, 10 μM, 1μM, and 0.1μM concentrations. Sample cells, like in the optimization step, underwent treatment both with and without 10 μM of CH-223191 inhibitor in addition to metabolite-specific treatments. Each metabolite was also directly compared to the AhR activity by TCDD. Vehicle controls of PBS and DMSO were also included in a dilution series. Cross-comparisons were made for each metabolite within their selected concentration gradients, between vehicle controls, and between TCDD. Data were analyzed using an ANOVA of 2-3 technical replicates per group in both Prism 9 and Microsoft Excel.

C. Luciferase Assay of p-Cresol Sulfate and TCDD, a Dual Metabolomic Effect

293T cells were cultured in DMEM High Glucose medium consisting of 10% FBS and 1% NaPy. Once confluent, cells were transfected at a concentration of 100 ng/μl as follows: lipofectamine was combined in a 1:1 ratio with the plasmids pAhR and pGud-Luc. The lipofectamine-plasmid complex was then added to the cells before an additional day of culture. Cells were then treated in the following three experimental groups: treatment with TCDD (100 nM, 10 nM, or 1 nM), treatment with p-cresol sulfate (100 μM, 10 μM, 1 μM, 0.1μM, or 0.01μM), or treatment with a combination of the two, where TCDD was held at a constant concentration of 10 nM (0.01 μM) and p-cresol was cross-titrated in the same 100 μM - 0.01 μM dilution series. After an additional 48 hours in culture, AhR activity was assessed using the Pierce Firefly Luciferase Glow Assay Kit (Thermo Fisher, USA). Cells were lysed for 5 minutes, followed by addition of D-Luciferin at 1:1000 in working solution. Luciferase activity was then measured using a luminometer set to measure absorbance at 480 nm. Data were analyzed using the same statistical methods in both Prism 9 and Microsoft Excel.

2. Culture of Primary T Cells and Assessment of Cytokine Production by Intracellular Cytokine Staining by Flow Cytometry and ELISA

Whole splenocyte populations were harvested from the spleen of 8–10-week-old B6 mice and stimulated for 72 hours with plate-bound anti-CD3 (5 μg/ml) under Th0 or Th17 (IL-1β, IL-23 TGFβ at 10ng/ml and IL-6 at 20ng/ml) conditions (**Fig. 4**). After 72 hours, cells were then stimulated with TCDD, p-cresol sulfate, or a combination of the 2 metabolites. The experimental groups mirrored those of part 3. Cells were treated with either 1 μM, 10 μM, or 100 μM of p-cresol sulfate,1 nM, 10 nM, or 100 nM of TCDD, or a combination of the two metabolites . The combined TCDD + p-cresol sulfate experimental group contained TCDD held at a concentration of 0.01 μM (10 nM), while p-cresol sulfate was experimentally tested down the concentration gradient of 100μM, 10μM, or 1μM. Cells were allowed to come to confluency over a 3-day period before being spun down at 21^{o}C at 1300RPM for the collection of the supernatant for downstream ELISA analysis. Cells were then stimulated with 20 ng/ml PMA, 1 μg/ml of ionomycin, and 1 mg/ml brefeldin A (Golgi Plug reagent) for 4 hours. Cells were then stained with a UV-Blue Live/Dead fixable stain (Thermo Fisher, USA) followed by surface staining with antibodies against CD45, CD11b, CD19, TCRβ, CD4, CD8, and TCRγδ. The respective stains used were Biolegend A700, APC-Fire, PE-Cy5, BV605, PE-DAZZLE, PE-Cy7, and APC (Biolegend, USA). For intracellular cytokine staining, cells were permeabilized with 0.05% saponin and stained with antibodies for IL-17 and IFN-γ (Biolegend PE and A647 stains, Biolegend USA). Cytokine levels of stained cells were analyzed using a Cytek Aurora (Cytek Biosciences, USA). The spectral unmixing was carried out with the help of suitable single-color controls and corrected for autofluorescence from a control group that was not stained. Data were then analyzed using FlowJo software (Version 10.8.1).

To run the ELISA (**Fig. 5**), a high-binding ELISA plate was coated with 100 μl of anti-mouse IL-17-A capture antibody (Biolegend, USA) diluted to 0.5 μg/ml in Coating Buffer (1.825g Na_2C0_3, 4.2g $NaHCO_3$ in 500 ml H_20, pH ~9.6) overnight at 4^{o}C. The plate was then blocked with ELISA Diluent (5% BCS in PBS) and washed with ELISA wash buffer (0.1% Tween in PBS) before adding the saved supernatants described above. After incubation overnight at 4^{o}C, the plate was washed 3 times before being exposed to biotin-labeled anti-mouse IL-17-A diluted to 0.5 μg/ml. After an hour of incubation and 3 more

washes, Avidin-HRP (0.1% in Diluent) was added to the plate. Samples were then incubated in the dark for half an hour before the addition of TMB (100µl/well). Samples were allowed to incubate until a blue color was seen (about 20 minutes). Once blue, stop solution (Thermofisher, USA) was added, and absorbance was read on a spectrophotometer at 450nm. Data were analyzed in both Prism 9 and Microsoft Excel by ANOVA with 3 technical replicates per group.

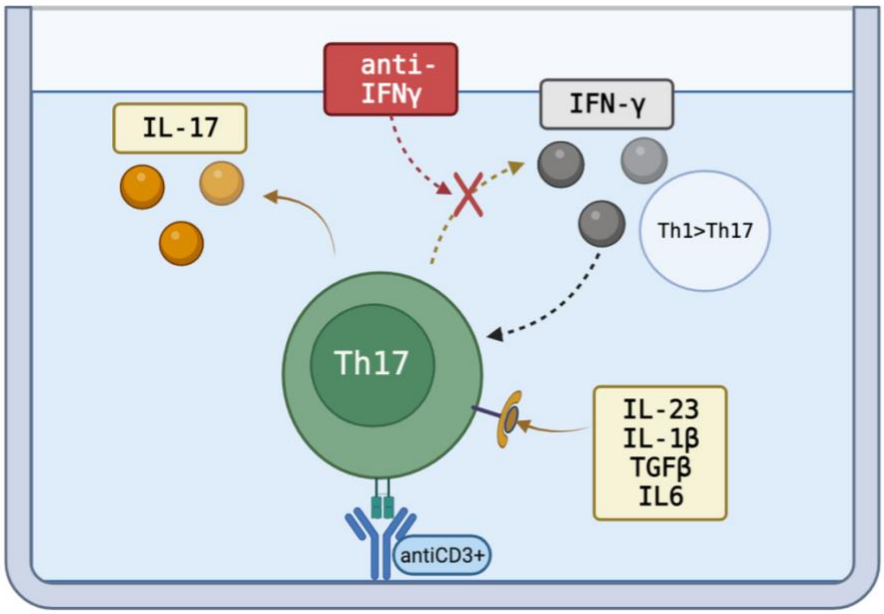

Figure 4. ***T Cell Differentiation of Th17 Phenotype***

Splenocytes were differentially polarized to Th0 (Th1) or Th17 phenotypes post-harvest. Both sets of cells were stimulated with plate-bound antiCD3^{+}, while Th17 polarization was done by stimulation with IL-1β, IL-23 TGFβ at 10ng/ml and IL-6 at 20ng/ml.

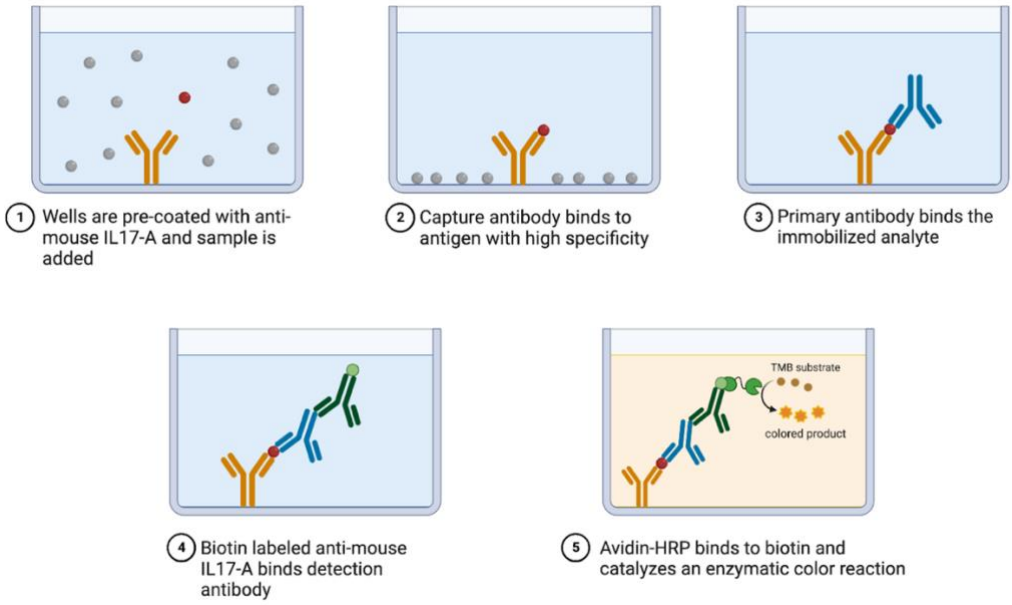

Figure 5. ***ELISA Setup for IL-17 Detection***

A depiction of the ELISA setup for IL-17 detection. Wells are pre-coated with anti-mouse IL17-A (Biolegend, USA) before binding to an antigen and analyte. A biotin labeled IL-17A (Biolegend, USA) is used for detection of IL-17 by an enzymatic reaction with Avidin-HRP (Biolegend, USA). IL-17 concentration is then measured comparatively between wells to an IL-17 standard (Biolegend, USA) by spectroscopy.

Results

1. Optimization of the Cell-based Luciferase Assay

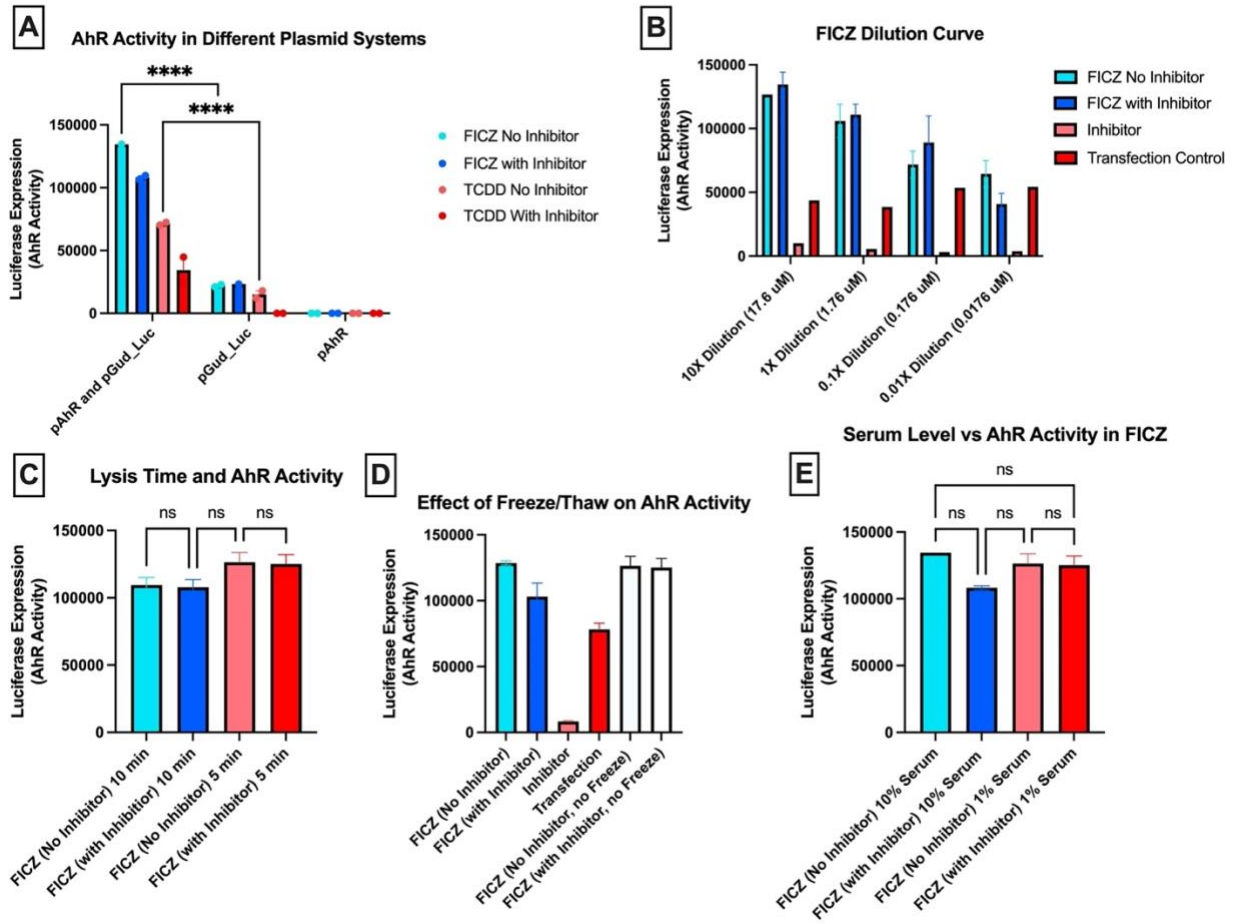

Figure 6. ***Optimization of AhR Luciferase Assay Reporter System***

Optimization of the luciferase assay used the known AhR agonists FICZ and TCDD. Agonists were first tested in (**A**) varying plasmid systems including pGud-Luc or pAhR alone or in combination and (**B**) using a dilution curve of FICZ (17.6 µM, 1.76 µM, 0.176 µM, and 0.0176 µM) in the optimal combined plasmid system. At each dilution factor, FICZ was tested both with and without the presence of the AhR inhibitor, CH-223191 and compared to a no-stimulus transfection control. Luciferase assay lysis time was evaluated comparing a 5 and 10-minute lysis time following treatment with FICZ at the highest concentration with and without CH-223191 (**C**). Effect of freezing supernatants after lysis (**D**) and the effect of serum level in the culture media (**E**) by comparing DMEM high Glucose medium with 10% FBS (10% serum) to DMEM High Glucose medium with 1% FBS (1% serum) were also examined. Error in each of the plots is represented by the standard error of the mean (SEM), with each condition repeated in technical triplicates.

To determine appropriate conditions for detecting bacterial metabolite driven AhR activation in a cell-based luciferase reporter assay, multiple faucets of the experimental protocol first needed to be optimized. Specifically, to examine the validity of the pGud-Luc plasmid in linking AhR activation to luciferase expression and to examine the relative contribution of the endogenous AhR expression in 293T cells as compared to that with pAhR plasmid encoded expression, various plasmid systems were tested (**Fig. 6A**). In testing the various plasmid systems, cells transfected with just pGud-Luc produced minimal AhR activity while those transfected with a combination of plasmids pAhR and pGud-Luc produced maximal AhR activity (**Fig. 6A**). Transfection with both plasmids was thus selected as the optimal plasmid system moving forward. Additionally, both FICZ and TCDD worked to produce AhR activity (**Fig. 6A**), supporting the validity of the assay. In order to test the functionally of the CH-223191 AhR inhibitor, an inhibitor condition was tested across plasmid systems. Both FICZ and TCDD were able to be inhibited by CH-223191 (**Fig. 6A)**, allowing for further downstream manipulation.

Additionally, to examine the potential effect of a dose responsive range of the assay, FICZ was tested both with and without the CH inhibitor down a dilution gradient (**Fig. 6B).** At the higher concentrations of 17.6 μM, 1.76 μM, and 0.176 μM, FICZ proved too strong an agonist to be inhibited by CH-223191. At these concentrations, induced AhR activity by FICZ was comparable with or without the presence of 10 μM CH-223191 (**Fig. 6B**). Moreover, in the same experiment, a transfection control was conducted to measure any potential basal endogenous AhR activity present in the cell without stimulation from an AhR agonist. As illustrated in **Figure 6B**, transfected cells even without an additional agonist present activated the AhR in minute levels. This endogenous activity, however, was consequently inhibited by the addition of CH-223191 **(Fig. 6B)**.

To determine if lysis time impacted maximal luciferase activity detection, we tested a 5 and 10-minute lysis time following treatment with FICZ, as shown in (**Fig. 6A**). In the presence of FICZ, with or without CH-223191 (10 μM), 5 minutes of lysis provided a greater AhR activity yield than a 10-minute lysis (**Fig. 6C**). As such, a 5-minute lysis time was used moving forward to yield maximal results. Additionally, in order to maximize the ability to complete more technical replicates without running into time constraints, the effect of freezing cells post-lysis was also examined (**Fig. 6D**). There was no significant

effect of freezing cells post-lysis (**Fig. 6D**). As such, freezing cells post lysis could be used to increase efficiency and the number of possible technical replicates on the same day of experimentation.

Levels of endogenous AhR activity present within the cell was of concern, as demonstrated by the transfection control in **Figure 6B**. In order to test whether this endogenous AhR activity was due to the serum in the DMEM High Glucose medium used for cell culture, and whether this endogenous activity could significantly impact results, the AhR activity of cells stimulated by FICZ was examined between cells in 10% and 1% FBS culture media. Given that no significant difference in AhR activity was measured between cells grown in either 10% or 1% FBS DMEM High Glucose (**Fig. 6E**), the standard 10% FBS was used moving forward. Taken together, these results established the optimal conditions for subsequent experiments and allowed for downstream applications of the luciferase assay.

2. Bacterial Metabolites Activate the AhR in a Cell-based Luciferase Assay

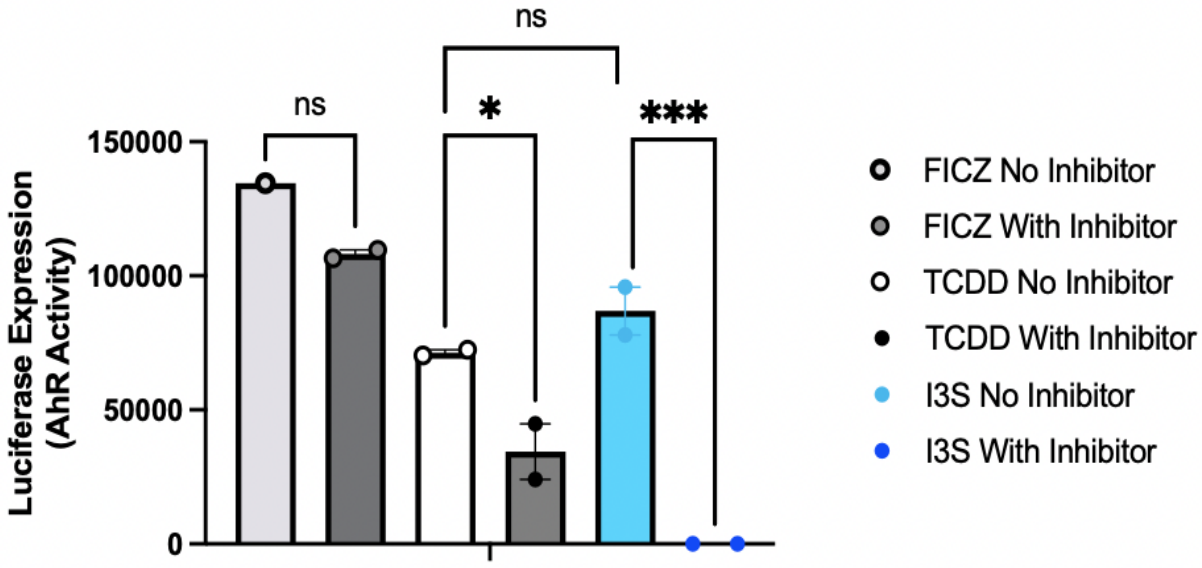

Figure 7. ***Comparison of Bacterial Metabolite I3S to Known AhR Agonists***

AhR activity via luciferase expression was analyzed for known AhR agonists TCDD (10 μM) and FICZ (10 μM) and known bacterial derived metabolite I3S at the same concentration (10 μM). Inhibition by CH-

223191 (10 μM) was also measured. Symbols indicate a significant difference between treatment groups as follows; *, $P \leq 0.05$; ***, $P < 0.001$; ns, not significant. The difference between TCDD and I3S was not significant ($p = 0.4877$). The difference between TCDD and TCDD with CH-223191 was significant ($p = 0.0189$). The difference between I3S and inhibited I3S was also significant ($p = 0.0001$). The differences between both FICZ groups was not significant ($p = 0.2008$). P values were calculated by a two-way ANOVA. Error was calculated by SEM with each condition repeated in technical replicates.

To evaluate whether tryptophan-dependent bacterial metabolite AhR activation can be measured in the optimized luciferase assay, the AhR activity of known agonists FICZ and TCDD was compared to that of a canonical bacterial metabolite, I3S. I3S, while bacterial in origin, is a tryptophan derivative of indoxyl processed by a mammalian host in the liver. Interestingly, I3S activated the AhR at comparable levels to TCDD ($P \leq 0.05$), a known and strong high affinity AhR agonist (**Fig. 7**). This indicates that I3S is a potent AhR agonist. On the other hand, TCDD and FICZ were only partially inhibited by CH-223191 while I3S was completely inhibited (**Fig. 7**), pointing to either ligand-specificity of CH-223191 or the potent strength of high affinity TCDD and FICZ. Moreover, as stipulated during the optimization stage of the assay, FICZ was unable to be inhibited by CH-223191. With or without the presence of CH-223191, FICZ strongly activated the AhR ($P \leq 0.05$) (**Fig. 7**). Taken together, these results highlight that bacterial metabolites can activate the AhR. Not to mention that the comparability between I3S and TCDD illustrates that bacterial metabolites can activate the AhR at comparable levels to known high-affinity agonists.

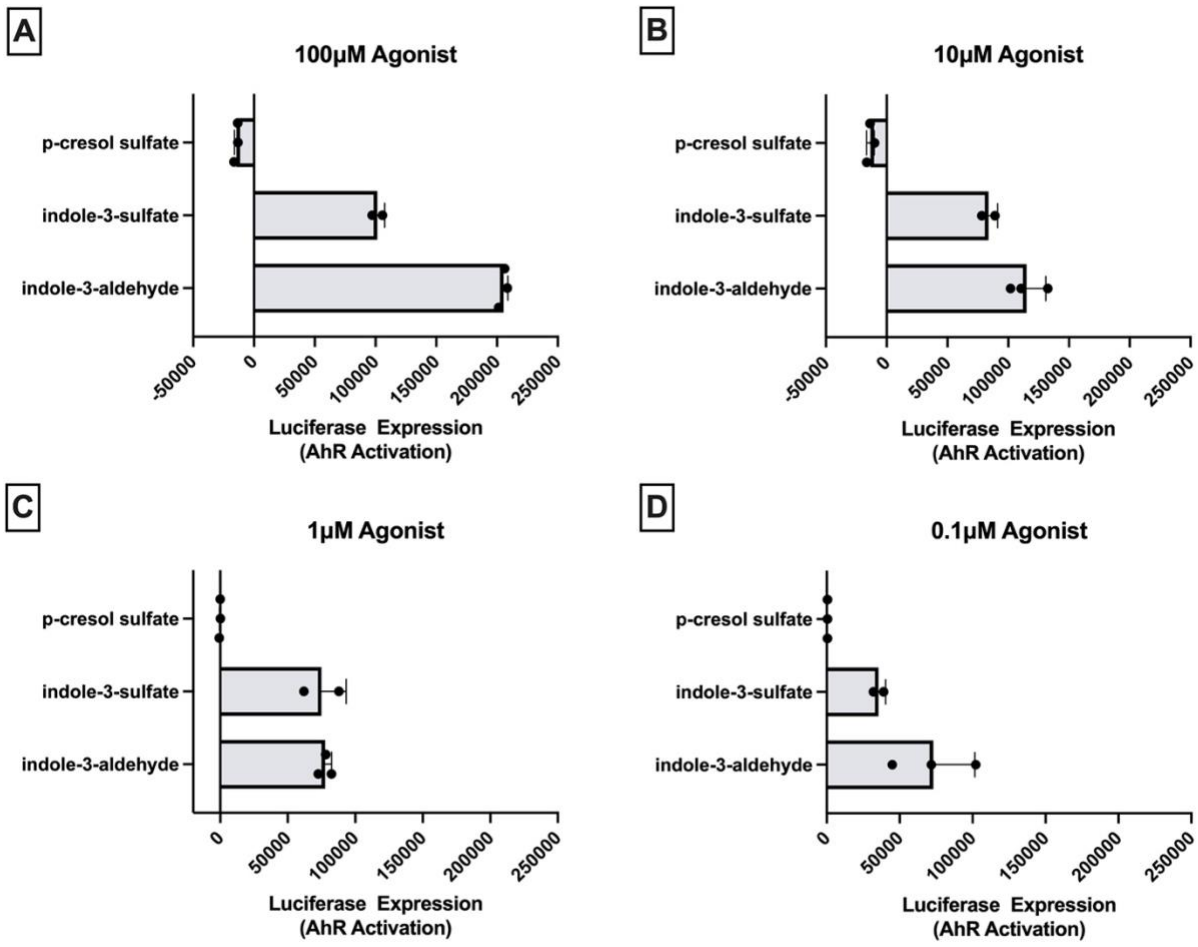

Figure 8. ***L. reuteri Derived Metabolites Activate the AhR***

Tryptophan-derived *L. reuteri* metabolites are sufficient to elicit AhR activation and do so in differing manners. Selected metabolites identified in *L. reuteri* monoculture including p-cresol sulfate and I3A, as well as known bacterial metabolite I3S, were analyzed in a cell-based luciferase assay at 100μM (**A**), 10μM (**B**), 1μM (**C**), and 0.1μM (**D**) concentrations for each individual metabolite. Data were normalized to AhR activation by DMSO vehicle controls. Error was calculated by SEM. All conditions were performed in triplicate.

To investigate the ability of *L. reuteri*-derived metabolites to activate the AhR, selected metabolites from *L. reuteri* monoculture, namely I3A and p-cresol sulfate, were compared to I3S, a known bacterial metabolite which had previously demonstrated to activate the AhR at a level comparable to high affinity agonists (**Fig. 7**). I3A and I3S both activated the AhR in a concentration-dependent fashion, where, in general, a higher concentration elicited a greater AhR response (**Fig. 8**). At the highest (100 μM)

concentration, I3A yielded nearly double the AhR activation of I3S (**Fig. 8A**). This suggests that when isolated, *L. reuteri* derived metabolites activate the AhR at comparable levels to known high affinity bacterial AhR agonists produced from similar tryptophan metabolic pathways (the bacterial indole pathway). At 1μM and 0.1 μM metabolite, however, AhR activation by I3S and I3A yielded no significant difference (**Fig. 8C**,**D**), suggesting a potential dose-dependent role. Nonetheless, even at 1μM and 0.1 μM, both I3S and I3A yielded a modest AhR response **(Fig. 8C,D)**.

Interestingly p-cresol sulfate exhibited modest AhR antagonistic activity at higher concentrations of 100 μM and 10 μM (**Fig. 8A**,**B**). This trend also continued with some minor inhibitory effects at 1 μM metabolite (**Fig. 8C**). At 0.1 μM metabolite, however, this inhibitory effect is no longer seen (**Fig. 8D**). Collectively, the strong activation by both I3S and I3A illustrates that tryptophan-derived *L. reuteri* metabolites elicit AhR response in a concentration-dependent manner equivalent to that of known agonists. The addition of potential inhibitory effects by p-cresol sulfate illustrates a dynamic and potentially divergent relationship between *L. reuteri*-produced metabolites and the AhR that is not straightforward.

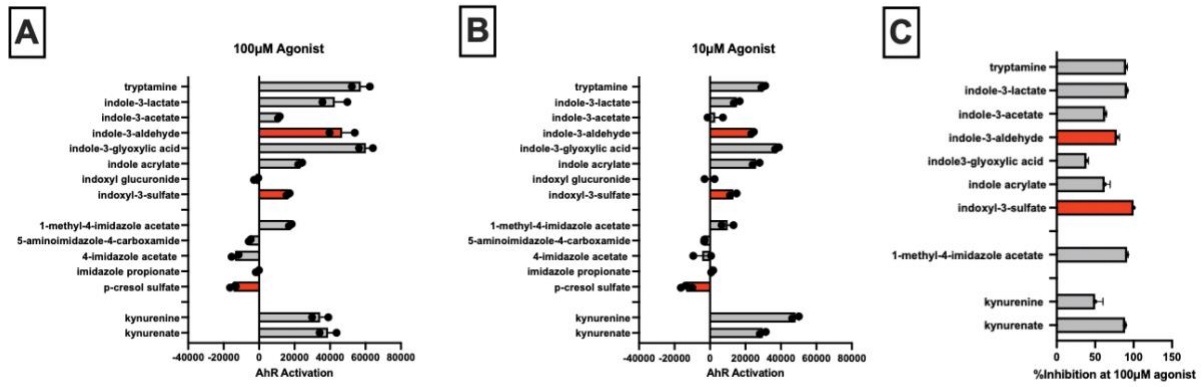

Figure 9. ***A Full Metabolic Profile of AhR Activity Induced by L. reuteri Metabolites***

A complete profile of all metabolites taken from *L. reuteri* monoculture data in a cell-based luciferase assay at 100 μM (**A**) and 10 μM (**B**) metabolite treatment that are sufficient to elicit AhR activation, including control bacterial metabolite I3S. Those highlighted in red were those I personally assayed, while those in grey were previously conducted in the Krementsov Lab [6]. The percent inhibition of AhR activation by CH-223191 in the presence of the indicated metabolites (**C**) was calculated between maximal luciferase response at 100μM and activity following pre-treatment with CH-223191 inhibitor.

To assess the potential of the full repertoire of tryptophan-associated metabolites produced by *L. reuteri* in monoculture to activate the AhR, each metabolite was examined at both 10 μM and 100 μM concentrations in the cell-based luciferase assay. Numerous *L. reuteri*-derived metabolites were shown to elicit a significant AhR response at both concentrations. Furthermore, metabolites of both the indole and mammalian kynurenate pathway of tryptophan metabolism were shown to activate the AhR (**Fig. 9**). Tryptamine, IGoxA, and I3A of the indole pathway, as well as both kynurenine and kynurenate of the kynurenine pathway evoked particularly strong AhR responses at a 100 μM concentration (**Fig. 9A**). Moreover, at a 10μM concentration, kynurenine induced the strongest response out of any metabolite (**Fig. 9B**).

Interestingly, many of the imidazole (derived from histidine metabolism) and cresol (classically tyrosine associated) metabolites elicited an AhR inhibitory effect rather than the predicted agonistic effect (**Fig. 9A**). Metabolites that elicited an inhibitory response included p-cresol sulfate, 5-aminoimidazole-4-carboxamide, 4-imidazole acetate, and imidazole propionate at 100 μM concentration (**Fig. 9A**). Additionally, p-cresol sulfate, 5-aminoimidazole-4-carboxamide, and 4-imidazole acetate also had inhibitory effects at a 10μM concentration (**Fig. 9B**). As previously seen in **Figure 6**, p-cresol sulfate elicited an inhibitory response, with magnitudes of -16000 at both 100 μM and 10 μM metabolite concentration (**Fig. 9A,B**). This inhibition of baseline AhR activity most likely represents inhibition of AhR ligands present in the culture media. This, in contrast to strong AhR agonistic activity by other metabolites, suggests a complex mechanism of regulation of AhR activity by *L. reuteri*-derived metabolites.

Additionally, to analyze the potential ligand specificity of the AhR and the ability of CH-223191 to inhibit these metabolites, percent inhibition by CH-223191 for each metabolite was calculated (**Fig. 9C**). Many strong AhR agonists, such as kynurenate and tryptamine, were nearly completely inhibited by CH-223191, with tryptamine having 90% inhibition and kynurenate having 88% inhibition (**Fig. 9C**). Other strong agonists like IGoxA, however, were only partially inhibited (**Fig. 9C**), suggesting high ligand specificity for the receptor and these metabolites. Taken together, these data illustrate the ability of *L.*

reuteri to produce both agonists and antagonists for the AhR and suggests a potential complex mechanism by which *L. reuteri* may impact immune response.

3. p-Cresol Sulfate Inhibits AhR activation by TCDD in a Cell-based Luciferase Assay

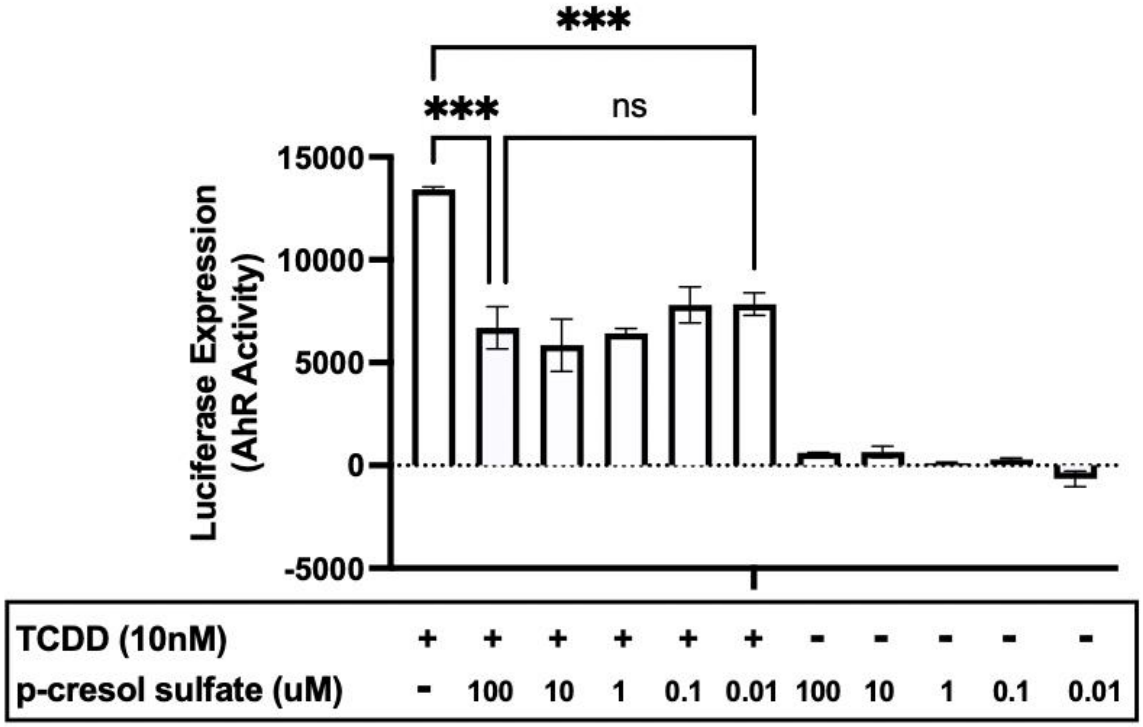

Figure 10. ***p-Cresol Sulfate is Sufficient to Inhibit TCDD Induced AhR Activity***

p-Cresol sulfate, a novel tryptophan-derived *L. reuteri* metabolite, is sufficient to inhibit AhR activity in a cell-based luciferase assay by TCDD, a known strong agonist to the receptor. AhR activity of TCDD at a 0.01 μM concentration was compared to that of a combination of TCDD (0.01 μM, constant) and p-cresol sulfate. The effects on TCDD by p-cresol sulfate was measured with varying concentration of p-cresol sulfate, including a series of 10-fold dilutions ranging from 100 μM to 0.01μM. P values were calculated by one-way ANOVA, the symbol *** represents $P < 0.001$, while “ns” represents a nonsignificant relationship ($P > .05$).

To determine if p-cresol sulfate AhR inhibition was sufficient to modulate receptor activation in response to strong agonist exposure, cells were pretreated with p-cresol

sulfate for 4 hours prior to exposure to the strong AhR agonist, TCDD. TCDD at a 10 nm (0.01 μM) concentration yielded significantly higher AhR activity ($P = 0.0001$) than was observed with 100 μM p-cresol sulfate pre-treatment (**Fig. 10**), suggesting that p-cresol sulfate indeed exerts an AhR inhibitory effect. In the presence of TCDD, AhR activity was even significantly inhibited at the lowest measured concentration of p-cresol sulfate (0.01μM), indicating that even a small quantity of p-cresol sulfate is sufficient to inhibit the AhR ($P = 0.0008$) (**Fig. 10**). Interestingly, the degree of inhibition by p-cresol sulfate did not appear to be concentration dependent ($P \leq 0.05$), with both 0.1μM and 100μM p-cresol sulfate pre-treatment exerting a similar inhibitory effect of TCDD mediated AhR activity (**Fig. 10**). The inhibitory action of p-cresol sulfate is more clearly seen when TCDD is used as a proxy for p-cresol inhibition, given that direct inhibitory effects of p-cresol sulfate on baseline AhR activity (**Fig. 9A,B**) are closer the limit of detection and are harder to tease out. This is also demonstrated when cells are only treated with p-cresol sulfate. These cells, produce inconsistent and close-to-baseline levels of AhR activation (**Fig. 10**). That having been said, these data demonstrate that p-cresol sulfate is sufficient to inhibit agonistic AhR activity by a high affinity proxy agonist, exhibiting its potential inhibitory strength.

4. p-Cresol Sulfate Decreases Cytokine Production in $CD4^+$, $CD8^+$, and TCRγδ T Cells by Flow Cytometry

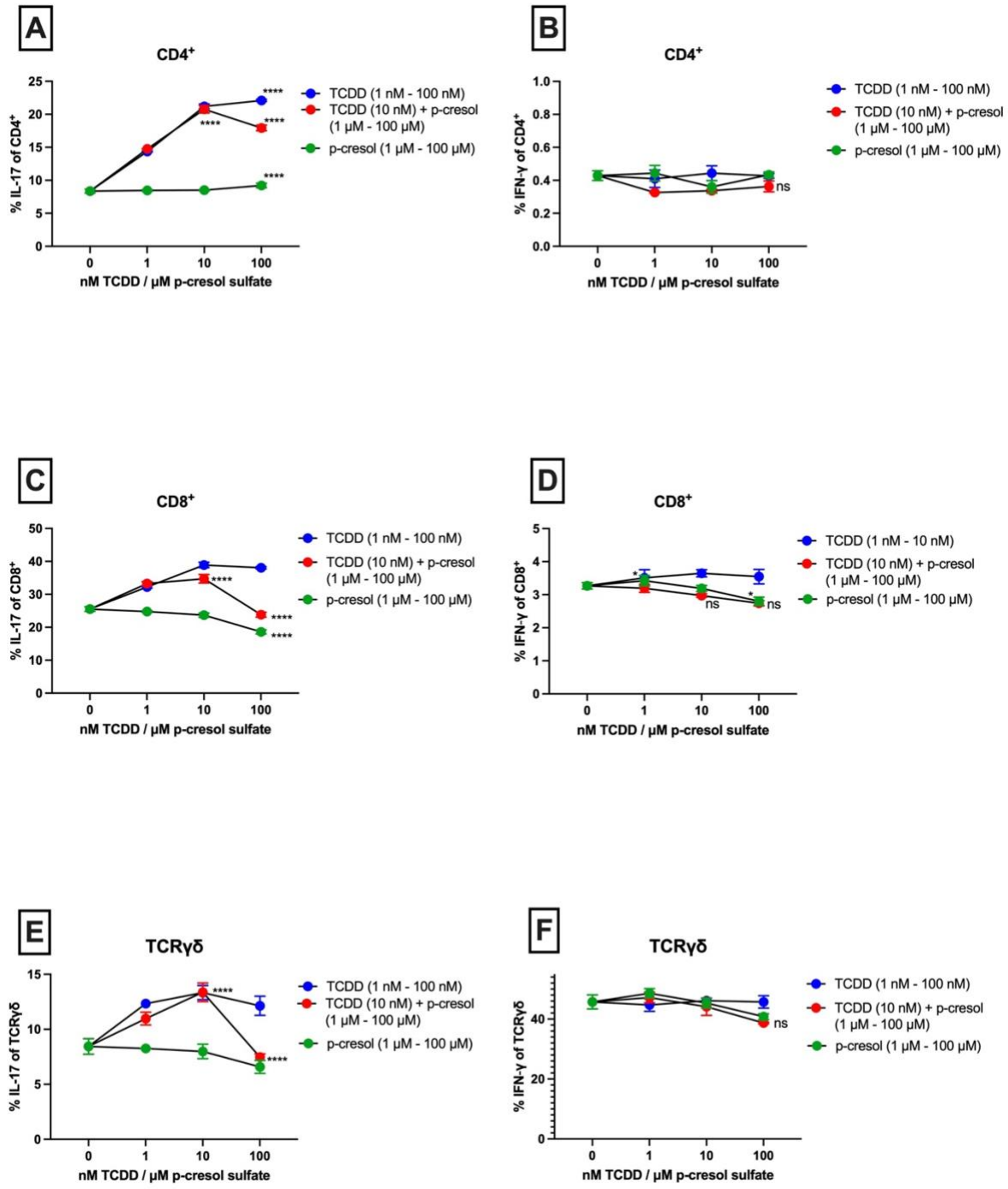

Figure 11. ***IL-17 and IFN-γ Cytokine Production of CD4⁺, CD8⁺, and TCRγδ T Cells by Flow Cytometry***
p-Cresol sulfate is sufficient to inhibit TCDD-induced AhR activity by flow cytometry in $CD4^+$, $CD8^+$, and TCRγδ T cells. Whole splenocytes were taken from 8–10-week-old B6 mice and were analyzed by flow cytometry for IL-17 and IFN-γ cytokine production. Splenocytes were differentiated under Th17 conditions for 72 hours and stimulated with 20 ng/ml PMA, 1 μg/ml of ionomycin, and 1 mg/ml brefeldin A (Golgi Plug reagent), with or without TCDD, p-cresol sulfate, or a combination of the two followed by intracellular cytokine staining and flow cytometry. Splenocytes were either stimulated with 1 μM, 10 μM, or 100 μM of p-cresol sulfate; 1 nM, 10 nM, or 100 nM of TCDD; or a combination of the two metabolites where TCDD is held at a constant 10 nM and p-cresol sulfate is titrated across it's concentration gradient of 1 μM, 10 μM, or 100 μM. Major effects of treatment include differences in percent IL-17 across treatment groups in $CD4^+$ (**A**), $CD8^+$ (**C**), and TCRγδ T cells (**E**). Percent IFN-γ was also examined in $CD4^+$ (**B**), $CD8^+$ (**D**), and TCRγδ T cells (**F**). Symbols indicate a significant difference between treatment groups at their given concentration as follows; ns, $P > 0.05$; *, $P \leq 0.05$; ****, $P < 0.0001$. P values were calculated by ANOVA, each result included at least 3 technical replicates.

The AhR is known to regulate the immune response in part by altering cytokine production through its function as a ligand activated transcription factor (REF). To determine if *L. reuteri*-derived AhR ligands can similarly affect immune cell cytokine production, flow cytometry was conducted on splenocytes stimulated with the high affinity agonist TCDD and *L. reuteri*-derived p-cresol sulfate in the same experimental set up as in **Figure 10.** Results from flow cytometry reinforced what was seen by the cell-based luciferase assay (**Fig. 11**; **Fig. 10**). In general, higher concentrations of TCDD increased IL-17 production in $CD4^+$ cells. 100 nM TCDD produced significantly higher IL-17 than 10 nM TCDD ($P < 0.0001$). Sequentially, 10 nM TCDD produced significantly higher IL-17 than 1 nM ($P < 0.0001$) (**Fig. 11A)**. TCDD, therefore, appears to increase IL-17 production in a concentration dependent manner. As TCDD is a known high-affinity AhR ligand, this demonstrates that AhR ligands can modulate cytokine production in primary T cells.

Conversely, in $CD4^+$ cells, p-Cresol sulfate did not increase IL-17 production beyond baseline levels (**Fig. 11A**). Additionally, an inhibitory effect of p-cresol sulfate was seen in the combined TCDD + p-cresol sulfate experimental condition. In $CD4^+$ cells, TCDD-driven IL-17 production was significantly inhibited by the addition of 100 μM p-cresol sulfate **(Fig. 11A**). This is demonstrated in the combined TCDD + p-cresol sulfate experimental condition, where cells stimulated with 100 μM p-cresol sulfate produced

significantly less IL-17 than cells stimulated with 10 μM p-cresol sulfate in the presence of TCDD ($P < 0.0001$) **(Fig. 11A**). Cells treated with 100 μM p-cresol sulfate and 10nM TCDD also produced less IL-17 than cells only stimulated with TCDD ($P < 0.0001$) **(Fig. 11A**), further illustrating that p-cresol sulfate has a concentration dependent inhibitory effect on IL-17 production.

On top of $CD4^+$ cells, this inhibitory effect of p-cresol sulfate was also observed in both $CD8^+$ and TCRγδ cells (**Fig. 11C,E**). In TCRγδ T cells, this inhibitory effect was only seen at a 100 μM concentration of p-cresol sulfate (**Fig. 11E**). This is illustrated in the combined TCDD + p-cresol sulfate experimental group, where TCRγδ cells stimulated with 100 μM p-cresol sulfate in the presence of 10 nM TCDD produced significantly less IL-17 than cells treated with just 10 nM TCDD ($P < 0.0001$) (**Fig. 11E**). Like in $CD4^+$ cells, this not seen at lower concentrations. In $CD8^+$ cells, however, p-cresol sulfate demonstrated a much stronger effect on IL-17 production. Like in $CD4^+$ and TCRγδ cells, the addition of 100 μM p-cresol sulfate to $CD8^+$ cells was sufficient to inhibit TCDD-driven IL-17 production. This is illustrated in the combined TCDD + p-cresol experimental group, where cells treated with 100 μM p-cresol sulfate produced less IL-17 than cells treated with 10 μM ($P < 0.0001$) (**Fig. 11C**). Unlike in $CD4^+$ or TCRγδ cells, however, an inhibitory effect of 10 μM p-cresol sulfate was also observed in $CD8^+$ cells. $CD8^+$ cells treated with 10 μM p-cresol sulfate and 10nM TCDD produced significantly less IL-17 than cells treated with just 10nM TCDD ($P = 0.0015$) (**Fig. 11C**). p-Cresol sulfate, therefore, appears to have a stronger inhibitory effect on IL-17 production in $CD8^+$ cells than in other T cell subsets.

Additionally, IFN-γ production was examined to determine if Th17 differentiated cells produce IFN-γ by treatment with TCDD or p-cresol sulfate, and if this treatment would have similar effects on IFN-γ to IL-I7. Unlike what is seen in IL-17, however, IFN-γ production is not affected by TCDD treatment in any cell subtype. In $CD4^+$, $CD8^+$, and TCRγδ cells, treatment with maximal TCDD (100 nM) did not produce significantly different amounts of IFN-γ than baseline levels ($P \geq 0.05$) (**Fig. 11B,D,F**). Additionally, treatment with maximal p-cresol sulfate (100 μM) did not change IFN-γ from baseline levels in $CD4^+$ or TCRγδ cells ($P \geq 0.05$) (**Fig. 11B,F**). Interestingly, however, there was a small effect of p-cresol sulfate on IFN-γ production in $CD8^+$ cells. $CD8^+$ cells treated with

100 μM p-cresol sulfate produced significantly less IFN-γ compared to those stimulated with 1 μM p-cresol sulfate ($P \leq 0.05$) (**Fig. 11D**), suggesting a potential concentration dependent inhibition of IFN-γ by p-cresol sulfate. Curiously, this effect was only seen when cells were treated with p-cresol sulfate not in the presence of TCDD. In the presence of TCDD, the addition of 100 μM p-cresol sulfate did not change IFN-γ production from baseline levels ($P \geq 0.05$) (**Fig. 11D**). Taken together, these data suggests that in Th17 differentiated $CD4^+$ and TCRγδ cells, treatment with AhR ligands TCDD and p-cresol sulfate is not sufficient to alter IFN-γ production. In $CD8^+$ cells, however, there may be a potential inhibitory effect of p-cresol sulfate treatment on IFN-γ. That having been said, this effect was modest and in general, p-Cresol sulfate had much stronger effects on IL-17 production. Taken together, these results highlight that *L. reuteri*-derived AhR ligands p-cresol sulfate and TCDD modulate IL-17 production in primary T cells.

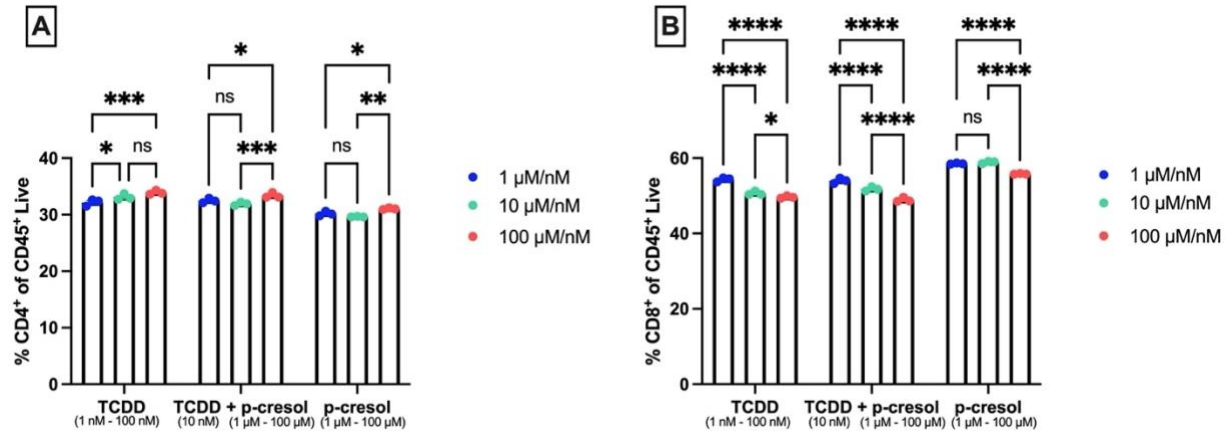

Figure 12. Effect of *L. reuteri* metabolite treatment on the *frequency of CD4⁺ and CD8⁺ T-Cells*

Splenocytes were taken from 8–10-week-old B6 mice and were analyzed by flow cytometry for IL-17 and IFN-γ cytokine production. Splenocytes were differentiated under Th17 conditions for 72 hours and stimulated with 20 ng/ml PMA, 1 μg/ml of ionomycin, and 1 mg/ml brefeldin A (Golgi Plug reagent), with or without TCDD, p-cresol sulfate, or a combination of the two followed by intracellular cytokine staining and flow cytometry. Splenocytes were either stimulated with 1 μM, 10 μM, or 100 μM of p-cresol sulfate; 1 nM, 10 nM, or 100 nM of TCDD; or a combination of the two metabolites where TCDD is held at a constant 10 nM and p-cresol sulfate is titrated across its concentration gradient of 1 μM, 10 μM, or 100 μM. The $\%CD4^+$ cells (**A**) and $\%CD8^+$ cells (**B**) of all $CD45^+$ leukocytes were calculated for each treatment condition. Symbols are as follows, *, $P \leq 0.05$; **, $P < 0.01$; ***, $P < 0.001$; ****, $P < 0.0001$. P values were calculated by ANOVA, each result included at least 3 technical replicates.

To determine if metabolite treatment impacted the proportion and proliferation of major T cell subsets, the %$CD4^+$ and %$CD8^+$ of total $CD45^+$ leukocytes was calculated. Interestingly, out of the total $CD45^+$ population, there were slightly more $CD4^+$ T cells upon treatment with 100 nM of TCDD than with 1 nM ($P < 0.001$) (**Fig. 12A**). This difference, however, while statistically significant, only accounted for only 1.7% of $CD4^+$ cells in the $CD45^+$ population. TCDD, therefore, may have a modest effect on $CD4^+$ cell proliferation at best. As TCDD is an AhR ligand, this effect on proliferation may also be AhR driven. Additionally, there were also slight differences in the proportion of $CD4^+$ cells in the $CD45^+$ population with treatment of p-cresol sulfate. Both with or without the presence of TCDD, treatment with 100 µM p-cresol sulfate had the highest proportion of $CD4^+$ cells in both p-cresol alone and p-cresol + TCDD experimental groups (**Fig. 12A**). Much like treatment with TCDD, however, this difference was modest. Any effect of p-cresol sulfate on $CD4^+$ proliferation is, therefore, also modest. Together, these results suggest that in $CD4^+$ cells, TCDD and p-cresol sulfate may have minor effects on cell proliferation that may potentially be AhR driven.

Additionally, there were some differences seen in the proportion of $CD8^+$ T cells with treatment by AhR agonists (**Fig. 12B**). In the TCDD (1 nM – 100 nM) condition, there was a higher proportion of cells stimulated with 1 nM TCDD than both 10 nM and 100 nM TCDD (**Fig. 12B**). This difference, however, while significant ($P \leq 0.05$), only accounts for 3.6% of the $CD8^+$ cells in the $CD45^+$ population between 1 nM and 10 nM TCDD. Any effect on $CD8^+$ proliferation caused by TCDD is, therefore, also modest. Much like TCDD, p-Cresol sulfate also had a mild effect on $CD8^+$ proliferation. In the combined TCDD + p-cresol sulfate experimental group, cells stimulated with 1 µM p-cresol sulfate accounted for significantly more of the $CD8^+$ population than cells treated with 100 µM (**Fig. 12B**). This difference, again while significant ($P < 0.0001$), accounts for only 5.1% of $CD8^+$ cells in the $CD45^+$ population and only suggests a mild effect of p-cresol sulfate on $CD8^+$ proliferation. Jointly, these results illustrate that TCDD and p-cresol sulfate may have a modest role in AhR driven cell proliferation, with a slightly stronger effect in $CD8^+$ than in $CD4^+$ cells.

5. Results by Flow Cytometry are not Mirrored by ELISA

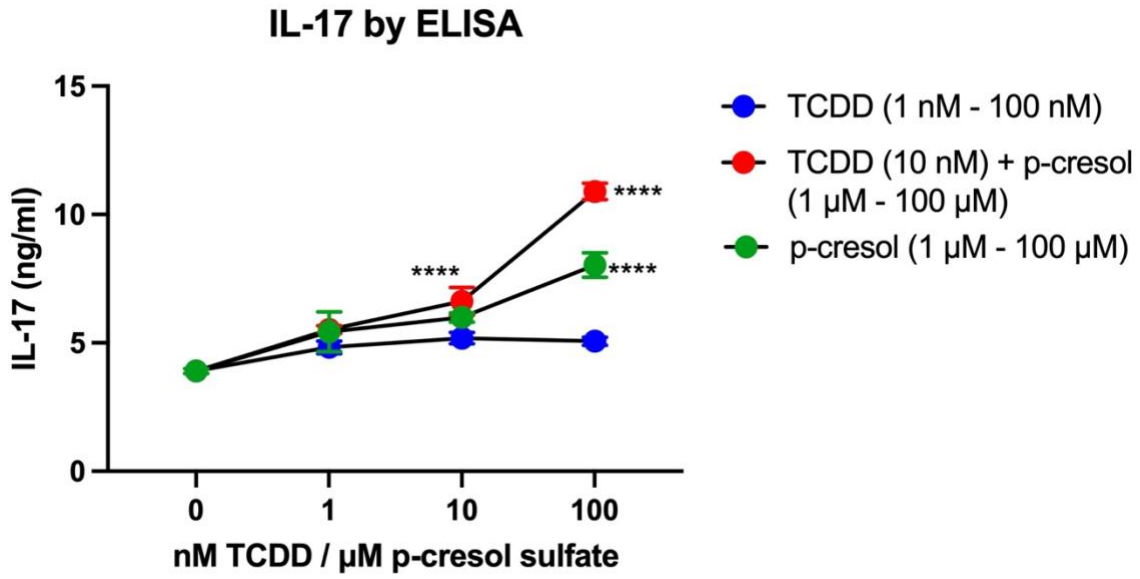

Figure 13. ***IL-17 Production by ELISA does not recapitulate cytokine measurement of flow cytometry***
Whole splenocyte populations were harvested from the spleen of 8–10-week-old B6 mice and stimulated with 1 µM, 10 µM, or 100 µM of p-cresol sulfate; 1 nM, 10 nM, or 100 nM of TCDD; or a combination of the two metabolites where TCDD is held at a constant 10 nM and p-cresol sulfate is titrated across its concentration gradient of 1 µM, 10 µM, or 100 µM. An ELISA measuring IL-17 (ng/mL) was then conducted on supernatants taken from cells following 3 days in culture. Symbols indicate a significant difference between treatment groups at their given concentration as follows; ****, $P < 0.0001$. P values were calculated by ANOVA, each result included at least 3 technical replicates.

To assess the effect of metabolite induced cytokine production through a parallel method to flow cytometry, the IL-17 production of splenocyte supernatants stimulated with TCDD and p-cresol sulfate were measured by ELISA. Generally, as measured by ELISA, metabolite driven IL-17 production opposed that of flow cytometry. Contrary to flow cytometry, where p-cresol sulfate inhibited TCDD driven IL-17 production in all cell types (**Fig. 11**), p-cresol sulfate appears to increase IL-17 production by ELISA (**Fig. 13**). By ELISA, treatment with 100 µM of p-cresol sulfate produced significantly more IL-17 than treatment with 10 µM or 1 µM ($P < 0.0001$). This would suggest a concentration dependent attenuative role of p-cresol sulfate in IL-17 production rather than the previously seen inhibitory role. Additionally, by ELISA p-cresol sulfate appeared to increase IL-17 in cells stimulated with TCDD. Cells stimulated with 10 nM TCDD and 100

μM p-cresol sulfate produced maximal IL-17, significantly more so than cells stimulated with 10 nM TCDD and 10 μM p-cresol sulfate ($P < 0.0001$) (**Fig. 13**). Interestingly, treatment with TCDD alone did not significantly increase IL-17 production beyond baseline levels (**Fig. 13**), almost mirroring the effect of the p-cresol sulfate condition by flow cytometry (**Fig. 11**). Together, these results would suggest that p-cresol sulfate increases IL-17 production while TCDD has no effect, the exact opposite conclusion of the results seen by flow cytometry (**Fig. 11**). Results by flow cytometry (**Fig. 11**) supported our hypothesis that that p-cresol sulfate, a hypothesized AhR antagonist, would decrease IL-17 production. ELISA, however, contradicted these results and our hypothesis. This ELISA data, therefore, highlights key assay differences between flow cytometry and ELISA.

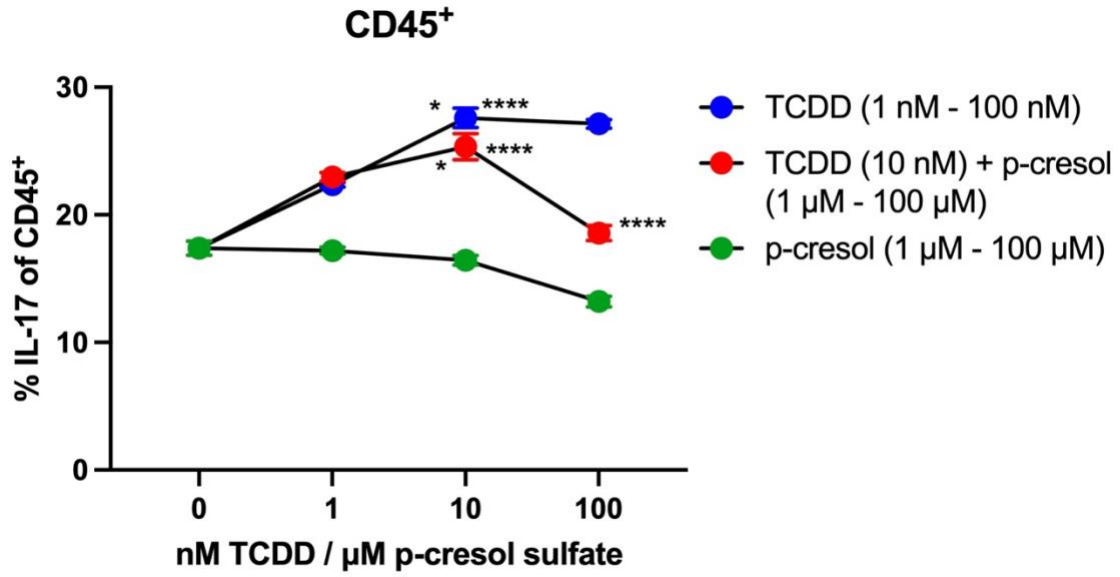

Figure 14. ***IL-17 Production of all CD45⁺Leukocytes by Flow Cytometry***

Whole splenocytes were taken from 8–10-week-old B6 mice and were analyzed by flow cytometry for IL-17 cytokine production. Splenocytes were differentiated under Th17 conditions with or without TCDD, p-cresol sulfate, or a combination of the two followed by intracellular cytokine staining and flow cytometry. Splenocytes were either stimulated with 1 μM, 10 μM, or 100 μM of p-cresol sulfate; 1 nM, 10 nM, or 100 nM of TCDD; or a combination of the two metabolites where TCDD is held at a constant 10 nM and p-cresol sulfate is titrated across it's concentration gradient of 1 μM, 10 μM, or 100 μM. The %IL-17 of all $CD45^+$ leukocytes was then analyzed by flow cytometry across each condition. Symbols indicate a significant difference between treatment groups at their given concentration as follows; *, $P \leq 0.05$; ****, $P < 0.0001$. P values were calculated by ANOVA, each result included at least 3 technical replicates.

To determine whether or not differing results by flow cytometry (**Fig. 11**) and by ELISA (**Fig. 13**) were caused by cytokine production of some ungated or otherwise unspecified cell type in flow cytometry analysis, the IL-17 production of all $CD45^+$ leukocytes by flow cytometry was analyzed. In all $CD45^+$ leukocytes, results mirror those seen in Figure 11, where TCDD increased IL-17 production in a concentration dependent manner (**Fig. 14**). In all $CD45^+$ leukocytes, cells stimulated with 10 nM TCDD produced significantly more IL-17 than cells stimulated with 1 nM TCDD ($P < 0.0001$) (**Fig. 14**). Additionally, cells stimulated with 100 μM p-cresol sulfate and 10 nM TCDD produced significantly less IL-17 than cells stimulated with 10 μM p-cresol sulfate and 10 nM TCDD ($P < 0.0001$) (**Fig. 14**), reinforcing the pattern seen in $CD4^+$, $CD8^+$, and TCRγδ cells where p-cresol sulfate demonstrated inhibitory action on TCDD-driven IL-17 production (**Fig. 11**). The inhibitory effects were also seen at 10 μM p-cresol sulfate, with cells stimulated with 10 μM p-cresol sulfate and 10 nM TCDD producing significantly less IL-17 than cells stimulated with just 10 nM TCDD ($P \leq 0.05$) (**Fig. 14**). This, again, suggests a strong inhibitory role for p-cresol sulfate in all $CD45^+$ leukocytes, not just gated $CD4^+$, $CD8^+$, and TCRγδ cells. Taken together, these data highlight that differences seen in IL-17 production between ELISA (**Fig. 13**) and flow cytometry (**Fig. 11**) aren't caused by gating scheme or IL-17 production of some unspecified cell population, but rather by differences in the assays themselves.

Table 2. ***Summary of Major Results***

A summary of major findings between the cell-based luciferase assay, flow cytometry, and ELISA. Results by luciferase are as follows; ++, extremely strong AhR agonist; +, strong AhR agonist; -, AhR antagonist; na, not assessed. Columns 3 and 4 illustrate results by flow cytometry and are expressed as IL-17 or IFN-γ production in $CD4^+$, $CD8^+$, and TCRγδ subsets. Column 5 illustrates IL-17 production in a whole splenocyte population differentiated under Th17 conditions. Symbols for flow cytometry and ELISA are as follows; +, increase in cytokine production; -, decrease in cytokine production; or no effect.

Metabolite Name	*Luciferase Assay*	*$CD4^+$/$CD8^+$/ TCRγδ IL-17* Production	*$CD4^+$/$CD8^+$/ TCRγδ IFN-γ* Production	*ELISA IL-17 Production*
FICZ	++	na	na	na
TCDD	+	+/+/+	No Effect	No Effect
I3S	+	na	na	na
I3A	+	na	na	na
p-Cresol sulfate	-	-/-/-	No Effect/-/No Effect	+

All major findings from the luciferase assay, flow cytometry, and ELISA are as shown in **Table 2**. I3A, a *L. reuteri*-derived metabolite activated the AhR in equivalent levels to I3S, a canonical bacterial metabolite of tryptophan metabolism, and TCDD, a known high-affinity agonist to the AhR (**Table 2**; **Fig. 7**; **Fig. 8**). p-Cresol sulfate, a novel *L. reuteri* metabolite from monoculture data [6] conversely acted as an AhR antagonist in the luciferase assay (**Table 2**; **Fig. 8**; **Fig. 9**; **Fig. 10**), illustrating a divergent and metabolite-specific action of *L. reuteri* metabolites at the receptor.

In general, metabolites that increased AhR activity in the luciferase assay also increased IL-17 production by flow cytometry, while AhR antagonists in the luciferase assay decreased cytokine production (**Table 2**). TCDD both activated the AhR in the luciferase assay as well as increased IL-17 production in all $CD4^+$, $CD8^+$, and TCRγδ subsets by flow cytometry (**Table 2**; **Figure 11**). TCDD, however, had no effect on IFN-γ (**Table 2**; **Figure 11**). p-Cresol sulfate, on the other hand, decreased AhR activity by the luciferase assay and decreased IL-17 production by flow cytometry in all T cell subsets. Interestingly, p-cresol sulfate also decreased IFN-γ production in $CD8^+$ cells (**Table 2**;

Fig. 11). Taken together, these data illustrate a parallel relationship between AhR activity by luciferase and cytokine production by flow cytometry, where a decrease in AhR activity by luciferase correlates to a decrease in IL-17 cytokine production by flow cytometry.

Results by flow cytometry, however, were not recapitulated by ELISA. TCDD, which increased AhR activity in the luciferase assay and increased IL-17 production by flow cytometry had no effect on IL-17 production by ELISA (**Table 2**; **Fig. 13**). Additionally, p-cresol sulfate, which decreased IL-17 production by flow cytometry, increased IL-17 production by ELISA (**Table 2**; **Fig. 13**). Collectively, these results highlight key assay differences between flow cytometry and ELISA with a need to replicate experimental findings to ultimately determine the role of p-cresol sulfate in impacting AhR-mediated cytokine production.

Discussion

Collectively, a cell-based luciferase assay was optimized and validated for high-throughput screening of the capacity for novel bacterial produced metabolites to activate the AhR. The pAhR/pGud-Luc dual plasmid system greatly boosted AhR expression from endogenous basal levels and could be quantified indirectly through luciferase activity (**Fig. 6**). Specifically, the AhR activity elicited by both FICZ and TCDD was much higher in the dual plasmid system than with pGud-Luc on its own (representing basal levels of endogenous AhR expression naturally present in 293T cells). This highlighted the need for both plasmids and was thus the plasmid system used moving forward (**Fig. 6A**). Lysis times and serum levels were particularly large concerns with this assay, as differences in these categories could impact AhR expression within the cell population and could potentially moderate results. The amount of FBS in the culture medium was especially concerning in its potential to moderate basal AhR expression but proved to cause negligible change (**Fig. 6E**).

Interestingly, a 5-minute cell-lysis time proved to yield slightly better results than the manufacturer suggested 10-minute lysis time and consequently 5-minutes of lysis was used moving forward (**Fig. 6C**). Dilution curves of both FICZ and TCDD responded well to the assay; however, FICZ proved too strong an agonist to be inhibited by CH-223191 (**Fig. 6B**). TCDD was thus the selected control agonist of choice moving forward. Previous work has shown that CH-223191 is a ligand-selective antagonist and preferentially works against halogenated aromatic hydrocarbons, such as TCDD [27], which is consistent with our observed failure of this antagonist to inhibit FICZ, which is a nitrogen heterocycle.

Once established, the luciferase assay proved valid not only in quantifying AhR activity by known agonists but also the AhR activity induced by novel *L. reuteri*-derived metabolites. I3A, one of the many *L. reuteri* metabolites produced in monoculture [6], activated the AhR at comparable levels to IS3 (**Fig. 8**), a classic bacterial metabolite that also activated the AhR comparably to TCDD (**Fig. 7**). I3S and I3A were even able to activate the AhR in small quantities of 1μM and 0.1μM concentrations (**Fig. 8C,D**). Moreover, many other metabolites from the kynurenine and indole pathways of tryptophan metabolism activated the AhR in varying levels (**Fig. 9A,B**). The amount of

AhR activation greatly varied between metabolites, with tryptamine and IGoxA eliciting the highest response at 100 μM and kynurenine at a 10 μM concentration. On the other hand, metabolites like indole-3-acetate and indoxyl glucuronide induced a much smaller AhR response. The AhR activation of indoxyl glucuronide, while present, was almost negligible compared to the more robust agonists (**Fig. 9A,B**). In combination, these data support our hypothesis that tryptophan-derived metabolites produced by *L. reuteri* act as agonists to the AhR, in some cases even comparably to high-affinity agonists like TCDD. This activation, however, is highly variable.

Many of the strong AhR agonists, such as tryptamine and kynurenate, were able to be nearly completely inhibited by CH-22319; while others, like IGoxA, were only partially inhibited (**Fig. 9C**). As CH-223191 is a known ligand-selective antagonist [27], the effect of CH-223191 on these metabolites, while not directly correlative with any immunologically important outcome, highlights the potential importance of ligand specificity of the AhR to consider. Many of these bacterial metabolites, such as I3A, are also aromatic hydrocarbons similar in structure to TCDD (**Fig. 2**). The effect of the AhR on autoimmunity is highly ligand-dependent, and ligand-specific responses can have drastic effects on immunological outcomes. For example, TCDD has been previously shown to have an attenuative effect on EAE in mouse models while other agonists like FICZ have been shown to cause EAE exacerbation [24]. Both of these agonists have been shown to bolster Th17 cell differentiation [24], and in our model, TCDD demonstrated an ability to increase IL-17 production (**Fig. 11**). Despite their similar effect on IL-17 and Th17 cell differentiation, they may have different immunological outcomes when taken into the context of an entire disease model. In combination, *L. reuteri*-derived metabolites not only activated the AhR in unique levels (**Fig. 9**) but also acted similar to these high affinity agonists in the cell-based luciferase assay (**Fig. 8**) and in flow cytometry (**Fig. 11**). As such, future study will be necessary to examine the individual effects of these metabolites in an EAE disease model.

The differing effects of *L. reuteri*-derived metabolites are further exhibited by the novel groups of imidazole and cresol metabolites, many of which had inhibitory effects on the AhR (**Fig. 9A,B**) contrary to our initial hypothesis. We found that p-cresol sulfate, a member of the bacterial cresols, is antagonistic to the AhR (**Fig. 8**; **Fig. 9**). Upon further

examination, we found that many metabolites of a novel imidazole group, including 5-aminoimidazole-4-carboxamide, 4-imidazole acetate, and imidazole propionate all had inhibitory effects on the AhR at a 100μM and 10μM concentration (**Fig. 9A,B**). Of these metabolites, however, p-cresol sulfate of the bacterial cresol group demonstrated a much more robust inhibitory effect than the others (**Fig. 9A,B**). That having been said, the results of p-cresol sulfate from the luciferase assay were inconsistent, and its antagonistic effect on the AhR was, at times, difficult to tease out due to the lower limit of detection of the assay. This is demonstrated in **Figure 10**, where p-cresol sulfate on its own only slightly inhibited AhR activity as compared to data shown in **Figures 8 and 9**, where p-cresol sulfate was a much stronger antagonist. The run-to-run variability in the luciferase assay for p-cresol sulfate was particularly high and could be a potential confounding variable to this study. Much of the inhibitory data was difficult to display in the luciferase assay as we continued to run into the lower limits of assay detection. By utilizing TCDD as a surrogate for a decrease in AhR activity upon the addition of p-cresol sulfate, however, this inhibitory effect was much easier to accentuate. When stimulated with TCDD and p-cresol sulfate, 293T cells in our model elicited much less AhR activity than compared to cells stimulated with just TCDD alone (**Fig. 10**). p-Cresol sulfate even produced AhR inhibition at a small concentration of 0.01 μM, indicating its potential strength as an AhR antagonist.

Along the lines of our hypothesis that AhR activity is paired to cytokine production, the inhibitory effect of p-cresol sulfate seen in the luciferase assay was paired with a decrease in IL-17 cytokine production by flow cytometry. IL-17 production was significantly inhibited by the addition of p-cresol sulfate to $CD4^+$, $CD8^+$, and TCRγδ cells stimulated with TCDD (**Fig. 11**). This inhibition was most strongly seen in $CD8^+$ cells (**Fig. 11C**). Interestingly, treatment with TCDD also led to a moderate increase in the proportion of $CD8^+$ cells (**Fig. 12**), a finding consistently found in MS patients [25,26]. $CD8^+$ cells also significantly produced less IFN-γ in the presence of p-cresol sulfate (**Fig. 11F**). Both IL-17 and IFN-γ are known to modulate disease pathogenesis in other EAE murine models [28]. As such, a decrease in either IL-17 or IFN-γ caused by p-cresol sulfate would result in an attenuation of disease state rather than exacerbation. In the initial EAE model, however, the introduction of *L. reuteri,* and subsequently it's metabolites, caused an

exacerbation of disease [6]. This could potentially be explained by the whole metabolomic environment. In a vacuum, p-cresol sulfate may decrease IL-17 production. On the other hand, other *L. reuteri*-derived metabolites, which may be more plentiful, have been shown to increase IL-17 production. For example, splenocytes exposed to IGoxA, which we show to be a strong AhR agonist (**Fig. 9**), has been shown to elicit an increase in IL-17 production in $CD4^+$ and $CD8^+$ subsets through flow cytometry [6]. In a vacuum, this would mean AhR activity by IGoxA increases pathogenic Th17 differentiation, and thus acts as a potential exacerbator of autoimmune disease. Taken together, the balance of multiple metabolites, and the net results of their unique effects most likely plays a much larger role in disease pathogenesis than any one individual metabolite.

We have shown data to suggest that AhR inhibition by p-cresol sulfate would seemingly have a role in the downregulation of pro-inflammatory Th17 and Th1 immune cells and would thus seemingly play some preventative role in autoimmune disease. Yet in MS patient sera, p-cresol has been found in elevated levels [29], suggesting some role in disease outcome. These two facts are seemingly contradictory. This harkens back to the notion of the total metabolomic environment, where the entire profile of metabolites creates a net effect on autoimmunity. It's possible that p-cresol sulfate, as a result of host *L. reuteri* tryptophan metabolism, is elevated in MS patient sera. The other metabolites created by *L. reuteri,* however, could be the cause of an exacerbated autoimmune phenotype. In our cell-based model, we found that many *L. reuteri*-derived metabolites are not only strong agonists for the AhR (**Fig. 9**), but also have the potential to impact inflammatory cytokine production (**Fig. 11**). Taken together, this suggests that *L. reuteri*-derived metabolites do indeed have the potential to impact disease state, and further highlights the need for more study to explain the effect of p-cresol sulfate in comparison to other metabolites.

The results surrounding the AhR in the literature are widely diverse and often contradict one another. The AhR seems to have a variable effect on autoimmunity dependent on its ligand. For example, high-affinity AhR agonists like TCDD and FICZ have divergent effects on autoimmunity; with TCDD ameliorating disease and FICZ exacerbating disease, even though both increase pro-inflammatory Th17 phenotypes in vitro [24]. It's also important to note that TCDD has an extremely long half-life and has

been found to elicit IL-17 production in $CD4^+$ cells 10 days post stimulation [31]. Conversely, FICZ is rapidly metabolized by the cell [31], pointing at some potential effect of duration as well as affinity to an autoimmune response. Moreover, induced AhR activity by the *L. reuteri*-derived metabolite kynurenine has been shown to support the generation of Tregs [32], while in our model, kynurenine boosted AhR activity (**Fig. 9**). By combining data from the luciferase assay and flow cytometry in our model however, an increase in AhR activity corresponded to an increase in pro-inflammatory IL-17 production. This is seen by TCDD, which both increased AhR activity in the luciferase assay (**Fig. 8**) and IL-17 production in flow cytometry (**Fig. 11**). In the context of autoimmune disease, the generation of Tregs seen by kynurenine [32] would be attenuative while IL-17 would exacerbate disease course. Again, these conflicting results point to the necessity for more study on the specific mechanism behind the AhR's role in autoimmune disease and any downstream applications to AhR activation.

Furthering the need for more study, a major limitation to the findings of this study is the mis-matching cytokine profiles by ELISA and flow cytometry. By flow cytometry and the cell-based luciferase assay, it appears that p-cresol sulfate inhibits AhR activity and consequent IL-17 production (**Fig. 8; Fig. 9; Fig. 11**). By ELISA, however, the exact opposite is true. ELISA data would suggest that the addition of p-cresol sulfate to TCDD seemingly increased IL-17 production rather than inhibiting it (**Fig. 13**). This would contradict other findings that p-cresol sulfate inhibited AhR activity (**Fig. 8; Fig 9**). One would expect that in order for p-cresol sulfate to increase IL-17 production, it would have to increase AhR activity if enhanced IL-17 production is occurring in an AhR dependent manner. Results by ELISA, therefore, are harder to believe and must be taken into the context of assay differences. While both ELISA and flow cytometry were used to measure IL-17 production in our model, these assays do so in a different manner. The ELISA simply measures all cytokines the entire cell population makes over a 3-day period of time in response to initial treatment with the AhR ligands. Flow cytometry, on the other hand, assesses the maximal possible cytokine production from stimulation with PMA, ionomycin, and brefeldin A. Differences in the assays themselves could simply explain the seemingly different cytokine production by the same cells. Nonetheless, results by ELISA provide questions and caveats to results of this study and repetition of both

experiments would be required to determine the precise role of p-cresol sulfate in modulating Th17 cytokine production.

One might also question if it's a cell-specific response of some ungated cell type in flow cytometry that caused differences that were observed by ELISA. Gating total lymphocytes present in flow cytometry samples, argues that this isn't the case. In $CD45^+$ cells, the addition of p-cresol inhibited AhR activity and IL-17 production by TCDD in the same fashion as in the $CD4^+$, $CD8^+$, and TCRγδ gated cell subsets (**Fig. 14**), suggesting that the results seen by ELISA aren't an artifact of differences in cytokine production between whole splenocyte populations and gated subsets.

Another caveat to our findings is the potential toxicity of p-cresol sulfate and TCDD. Both of these AhR ligands are known to be cellularly toxic [33, 34], and their potential effects on cell number could be a confounding variable to our results. We, however, didn't see a dramatic effect on the frequency of live $CD45^+$ leukocytes by either of these ligands **(Fig. 12**). An increase in p-cresol at 100 μM did decrease $CD8^+$ frequency in the total $CD45^+$ live population (**Fig. 12**), however, this effect was minute. This effect was also not seen in other cell types and flow data of the entire $CD45^+$ mimicked the results of individual cell types (**Fig. 14**), indicating that these results in $CD8^+$ were minor and ligand toxicity didn't impact the population of cells as a whole. We also didn't find any indication of toxicity of either ligand in the cell-based luciferase assay, illustrating that cell toxicity didn't play a major role in skewing results.

Collectively, our data show that *L. reuteri*, which has been previously shown to exacerbate EAE disease models [5,6], produces tryptophan-derived metabolites that act as ligands to the AhR. These ligands, however, act differentially at the AhR. Some are strong agonists, like IGoxA, which have been shown to increase IL-17 production in splenocyte populations [6]. While others, like p-cresol sulfate, conversely act as antagonists to the AhR. In vitro, AhR inhibitory action by p-cresol sulfate has shown to decease IL-17 production. While a decrease in IL-17 may suggest a neuroprotective role of p-cresol, the entire array of metabolites produced by *L. reuteri*, as well as environmental contexts, must be considered. The intensifying effect on EAE by *L. reuteri* is most likely the caused by net sum of many environmental and metabolite effects on the AhR, including any potential metabolomic effects from other microbiota in the gut. When looking

at the role of *L. reuteri* and the potential role of its metabolites on autoimmunity, it's niche in the entire gut microbiome environment must be considered. These findings ultimately lead to the need for more study on the role of the AhR and how it may impact autoimmune disease. More study is needed to define the exact mechanisms of the AhR signaling pathway which lead to the divergent findings of this study and to its impact on the immune system.

Conclusion

In conclusion, we found that a host of metabolites derived from tryptophan metabolism in *L. reuteri* act as ligands to the AhR, an important immunomodulatory receptor in the context of MS and autoimmune disease. As such, we propose a potential mechanism by which *L. reuteri* may foster autoimmunity and autoimmune disease. Analysis of *L. reuteri*-derived metabolites found that metabolites act divergently at the AhR, with some causing agonistic AhR activity while others suppress the receptor. Together with other studies on novel microbiota-immune interactions, we suggest that bacterial metabolites as mechanistically impacting the AhR signaling cascade may be a crucial component as to how commensal microbiota like *L. reuteri* modulate the immune system and exacerbate autoimmune disease. More study is needed to define the role of the AhR signaling pathway in autoimmunity and to define the exact mechanisms that trigger contrasting metabolite specific effects on the AhR.

References

1. Walton, C., King, R., Rechtman, L., Kaye, W., Leray, E., Marrie, R. A., Robertson, N., La Rocca, N., Uitdehaag, B., van der Mei, I., Wallin, M., Helme, A., Angood Napier, C., Rijke, N., & Baneke, P. (2020). Rising prevalence of multiple sclerosis worldwide: Insights from the Atlas of MS, third edition. Multiple sclerosis (Houndmills, Basingstoke, England), 26(14), 1816–1821. https://doi.org/10.1177/1352458520970841

2. Lucchinetti, C., Brück, W., Parisi, J., Scheithauer, B., Rodriguez, M., & Lassmann, H. (2000). Heterogeneity of multiple sclerosis lesions: implications for the pathogenesis of demyelination. Annals of neurology, 47(6), 707–717. https://doi.org/10.1002/1531-8249(200006)47:6<707::aid-ana3>3.0.co;2-q

3. Luchicchi, A., Preziosa, P., & Hart, B. (2021). Editorial: "Inside-Out" vs "Outside-In" Paradigms in Multiple Sclerosis Etiopathogenesis. Frontiers in cellular neuroscience, 15, 666529. https://doi.org/10.3389/fncel.2021.666529

4. Crayton, H. J., & Rossman, H. S. (2006). Managing the symptoms of multiple sclerosis: A multimodal approach. Clinical Therapeutics, 28(4), 445-60. https://doi.org/10.1016/j.clinthera.2006.04.005

5. Montgomery, T. L., Künstner, A., Kennedy, J. J., Fang, Q., Asarian, L., Culp-Hill, R., D'Alessandro, A., Teuscher, C., Busch, H., & Krementsov, D. N. (2020). Interactions between host genetics and gut microbiota determine susceptibility to CNS autoimmunity. Proceedings of the National Academy of Sciences of the United States of America, 117(44), 27516–27527. https://doi.org/10.1073/pnas.2002817117

6. Montgomery, T. L., Eckstrom, K., Lile, K. H., Caldwell, S., Heney, E. R., Lahue, K. G., D'Alessandro, A., Wargo, M. J., & Krementsov, D. N. (2022). Lactobacillus reuteri tryptophan metabolism promotes host susceptibility to CNS autoimmunity. Microbiome, 10(1), 198. https://doi.org/10.1186/s40168-022-01408-7

7. Gaetani, L., Boscaro, F., Pieraccini, G., Calabresi, P., Romani, L., Di Filippo, M., & Zelante, T. (2020). Host and Microbial Tryptophan Metabolic Profiling in Multiple Sclerosis. Frontiers in Immunology, 11. https://doi.org/10.3389/fimmu.2020.00157

8. Fine, R. L., Mubiru, D. L., & Kriegel, M. A. (2020). Friend or foe? lactobacillus in the context of autoimmune disease. Advances in Immunology, 29–56. https://doi.org/10.1016/bs.ai.2020.02.002

9. He, B., Hoang, T. K., Tian, X., Taylor, C. M., Blanchard, E., Luo, M., Bhattacharjee, M. B., Freeborn, J., Park, S., Couturier, J., Lindsey, J. W., Tran, D. Q., Rhoads, J. M., & Liu, Y. (2019). Lactobacillus reuteri Reduces the Severity of Experimental Autoimmune Encephalomyelitis in Mice by Modulating Gut Microbiota. Frontiers in immunology, 10, 385. https://doi.org/10.3389/fimmu.2019.00385

10. Johanson, D. M., 2nd, Goertz, J. E., Marin, I. A., Costello, J., Overall, C. C., & Gaultier, A. (2020). Experimental autoimmune encephalomyelitis is associated with changes of the microbiota composition in the gastrointestinal tract. Scientific reports, 10(1), 15183. https://doi.org/10.1038/s41598-020-72197-y

11. Gutiérrez-Vázquez, C., & Quintana, F. J. (2018). Regulation of the Immune Response by the Aryl Hydrocarbon Receptor. Immunity, 48(1), 19–33. https://doi.org/10.1016/j.immuni.2017.12.012

12. Logsdon, A. F., Erickson, M. A., Rhea, E. M., Salameh, T. S., & Banks, W. A. (2017). Gut reactions: How the blood–brain barrier connects the microbiome and the brain. Experimental Biology and Medicine, 243(2), 159–165. https://doi.org/10.1177/1535370217743766

13. Marinelli, L., Martin-Gallausiaux, C., Bourhis, J. M., Béguet-Crespel, F., Blottière, H. M., & Lapaque, N. (2019). Identification of the novel role of butyrate as AhR ligand in human intestinal epithelial cells. Scientific reports, 9(1), 643. https://doi.org/10.1038/s41598-018-37019-2

14. Zelante, T., Iannitti, R. G., Cunha, C., De Luca, A., Giovannini, G., Pieraccini, G., Zecchi, R., D'Angelo, C., Massi-Benedetti, C., Fallarino, F., Carvalho, A., Puccetti, P., & Romani, L. (2013). Tryptophan catabolites from microbiota engage aryl hydrocarbon receptor and balance mucosal reactivity via interleukin-22. Immunity, 39(2), 372–385. https://doi.org/10.1016/j.immuni.2013.08.003

15. Rejdak, K., Petzold, A., Kocki, T., Kurzepa, J., Grieb, P., Turski, W. A., & Stelmasiak, Z. (2007). Astrocytic activation in relation to inflammatory markers during clinical exacerbation of relapsing-remitting multiple sclerosis. Journal of neural transmission (Vienna, Austria : 1996), 114(8), 1011–1015. https://doi.org/10.1007/s00702-007-0667-y

16. Hartai, Z., Klivenyi, P., Janaky, T., Penke, B., Dux, L., & Vecsei, L. (2005). Kynurenine metabolism in multiple sclerosis. Acta neurologica Scandinavica, 112(2), 93–96. https://doi.org/10.1111/j.1600-0404.2005.00442.x

17. Kepplinger, B., Baran, H., Kainz, A., Ferraz-Leite, H., Newcombe, J., & Kalina, P. (2005). Age-related increase of kynurenic acid in human cerebrospinal fluid - IgG and beta2-microglobulin changes. Neuro-Signals, 14(3), 126–135. https://doi.org/10.1159/000086295

18. Routy, J. P., Routy, B., Graziani, G. M., & Mehraj, V. (2016). The Kynurenine Pathway Is a Double-Edged Sword in Immune-Privileged Sites and in Cancer: Implications for Immunotherapy. International journal of tryptophan research : IJTR, 9, 67–77. https://doi.org/10.4137/IJTR.S38355

19. Rothhammer, V., Borucki, D. M., Garcia Sanchez, M. I., Mazzola, M. A., Hemond, C. C., Regev, K., Paul, A., Kivisäkk, P., Bakshi, R., Izquierdo, G., Weiner, H. L., & Quintana, F. J. (2017). Dynamic regulation of serum aryl hydrocarbon receptor agonists in MS. Neurology(R) neuroimmunology & neuroinflammation, 4(4), e359. https://doi.org/10.1212/NXI.0000000000000359

20. Baĭdina, T. V., Akintseva, I.uV., & Trushnikova, T. N. (2014). Sindrom khronicheskoĭ ustalosti u bol'nykh rasseiannym sklerozom i soderzhanie serotonina v trombotsitakh periphericheskoĭ krovi [A chronic fatigue syndrome and blood platelet serotonin levels in patients with multiple sclerosis]. Zhurnal nevrologii i psikhiatrii imeni S.S. Korsakova, 114(2 Pt 2),

21. Baidina, T. V., Trushnikova, T. N., & Danilova, M. A. (2018). Interferon-indutsirovannaia depressiia i soderzhanie serotonina v periphericheskoĭ krovi u bol'nykh rasseiannym sklerozom [Interferon-induced depression and peripheral blood serotonin in patients with multiple sclerosis]. Zhurnal nevrologii i psikhiatrii imeni S.S. Korsakova, 118(8. Vyp. 2), 77–81. https://doi.org/10.17116/jnevro201811808277

22. Levi, I., Gurevich, M., Perlman, G., Magalashvili, D., Menascu, S., Bar, N., Godneva, A., Zahavi, L., Chermon, D., Kosower, N., Wolf, B. C., Malka, G., Lotan-Pompan, M., Weinberger, A., Yirmiya, E., Rothschild, D., Leviatan, S., Tsur, A., Didkin, M., Dreyer, S., … Segal, E. (2021). Potential role of indolelactate and butyrate in multiple

sclerosis revealed by integrated microbiome-metabolome analysis. Cell reports. Medicine, 2(4), 100246. https://doi.org/10.1016/j.xcrm.2021.10024

23. Herman, S., Åkerfeldt, T., Spjuth, O., Burman, J., & Kultima, K. (2019). Biochemical Differences in Cerebrospinal Fluid between Secondary Progressive and Relapsing–Remitting Multiple Sclerosis. Cells, 8(2), 84. https://doi.org/10.3390/cells8020084

24. Quintana, F. J., Basso, A. S., Iglesias, A. H., Korn, T., Farez, M. F., Bettelli, E., Caccamo, M., Oukka, M., & Weiner, H. L. (2008). Control of T(reg) and T(H)17 cell differentiation by the aryl hydrocarbon receptor. Nature, 453(7191), 65–71. https://doi.org/10.1038/nature06880

25. Friese, M. A., & Fugger, L. (2009). Pathogenic CD8+ T cells in multiple sclerosis. Annals of Neurology, 66(2), 132–141. https://doi.org/10.1002/ana.21744

26. Friese, M. A., & Fugger, L. (2005). Autoreactive CD8+ T cells in multiple sclerosis: A new target for therapy? Brain, 128(8), 1747–1763. https://doi.org/10.1093/brain/awh578

27. Zhao, B., Degroot, D. E., Hayashi, A., He, G., & Denison, M. S. (2010). CH223191 is a ligand-selective antagonist of the Ah (Dioxin) receptor. Toxicological sciences : an official journal of the Society of Toxicology, 117(2), 393–403. https://doi.org/10.1093/toxsci/kfq217

28. El-behi, M., Rostami, A. & Ciric, B. Current Views on the Roles of Th1 and Th17 Cells in Experimental Autoimmune Encephalomyelitis. J Neuroimmune Pharmacol 5, 189–197 (2010). https://doi-org.ezproxy.uvm.edu/10.1007/s11481-009-9188-9

29. Ntranos, A., Park, H. J., Wentling, M., Tolstikov, V., Amatruda, M., Inbar, B., Kim-Schulze, S., Frazier, C., Button, J., Kiebish, M. A., Lublin, F., Edwards, K., & Casaccia, P. (2022). Bacterial neurotoxic metabolites in multiple sclerosis cerebrospinal fluid and plasma. Brain : a journal of neurology, 145(2), 569–583. https://doi.org/10.1093/brain/awab320

30. Veldhoen, M., Hirota, K., Christensen, J., O'Garra, A., & Stockinger, B. (2009). Natural agonists for aryl hydrocarbon receptor in culture medium are essential for optimal differentiation of Th17 T cells. The Journal of experimental medicine, 206(1), 43–49. https://doi.org/10.1084/jem.20081438

31. Ehrlich, A. K., Pennington, J. M., Bisson, W. H., Kolluri, S. K., & Kerkvliet, N. I. (2018). TCDD, FICZ, and Other High Affinity AhR Ligands Dose-Dependently Determine the Fate of CD4+ T Cell Differentiation. Toxicological sciences : an official journal of the Society of Toxicology, 161(2), 310–320. https://doi.org/10.1093/toxsci/kfx215

32. Mezrich, J. D., Fechner, J. H., Zhang, X., Johnson, B. P., Burlingham, W. J., & Bradfield, C. A. (2010). An interaction between kynurenine and the aryl hydrocarbon receptor can generate regulatory T cells. Journal of immunology (Baltimore, Md. : 1950), 185(6), 3190–3198. https://doi.org/10.4049/jimmunol.0903670

33. Liu, W.-C., Tomino, Y., & Lu, K.-C. (2018). Impacts of Indoxyl Sulfate and p-Cresol Sulfate on Chronic Kidney Disease and Mitigating Effects of AST-120. Toxins, 10(9), 367. https://doi.org/10.3390/toxins10090367

34. Stohs, S. J. (1990). Oxidative stress induced by 2,3,7,8-tetrachlorodibenzo-p-dioxin (TCDD). *Free Radical Biology and Medicine*, *9*(1), 79– 90. https://doi.org/10.1016/0891-5849(90)90052-k